Sapienza University, Rome

Department of Human

Neuroscience PhD program

in

Innovative Technologies In Diseases Of

Skeleton, Skin And Oro-Craniofacial District

PhD program director: **Prof. Diego Ribuffo**

PhD project supervisor: **Prof. Andrea Truini**

Changing perspectives: from neurophysiology to nerve ultrasound

Candidate:

Dr. Giuseppe Di Pietro

Academic year: 2023-2024

ABSTRACT

BACKGROUND

Neuromuscular disorders impose significant challenges on individuals, their caregivers, and the healthcare systems. These conditions frequently stem from genetic factors, involve progressive degeneration, and affect life quality.

In the Neuromuscular Unit the diagnostic work-up mainly relies on clinical and neurophysiological assessment.

In the last years, high-resolution ultrasound examination of the Peripheral Nervous System has increasingly gained recognition as a complementary method finding numerous applications. This technique is able to provide useful information for the diagnosis and treatment of neuromuscular diseases.

AIM

This study series aims primarily to define the utility of nerve ultrasound in specific neuromuscular diseases, determining its feasibility and field of application.

Secondly, it aims to investigate the association between clinical, neurophysiological and neurosonological findings.

RESULTS

Study 1 - Predicting value for incomplete recovery in Bell's palsy of facial nerve ultrasound versus nerve conduction study.

We prospectively enrolled 34 patients with Bell's palsy. All patients underwent neurophysiological testing and High-resolution Ultrasound (HRUS) of the facial nerve at 10-15 days (T1), one month (T2), and three months (T3) after the onset of Bell's palsy. We have then compared the accuracy of HRUS with that of the facial nerve conduction study in predicting incomplete clinical recovery at three and six months. We found that in the first days after Bell's palsy onset, the diameter of the affected facial nerve is increased compared with the normal side, thus potentially enhancing the diagnostic assessment. The negative predictive value of a facial nerve diameter asymmetry of 25 % was relatively high (i.e., 94.73 %). Accordingly, we may speculate that an asymmetry lower than this threshold might be sensitive in detecting patients with a high probability of complete recovery.

However, facial nerve HRUS examination has a poorer prognostic value than facial nerve conduction study in patients with Bell's palsy.

Study 2 - Nerve Ultrasound in Friedreich's Ataxia: enlarged nerves as a biomarker of disease severity.

Ten patients diagnosed with Friedreich's Ataxia underwent an extensive clinical evaluation (SARA, FARS, mFARS, INCAT, ADL 0-36, IADL). Furthermore, they underwent nerve conduction study and nerve ultrasound. The assessment of nerve cross-sectional area, performed at 24 nerve sites, was compared to data collected from 20 healthy volunteers. All the patients had a severe sensory axonal neuropathy. HRUS showed a significant enlargement of median and ulnar nerves at the axilla and arm. The cumulative count of affected nerve sites was directly associated with clinical disability scales. Nerve ultrasound can offer valuable insights in cases where nerve conduction studies yield limited information. Nerve ultrasound is a potential biomarker of disease severity in Friedreich's ataxia.

Study 3 – Muscle ultrasound in Inclusion Body Myositis.

We compared echo intensity (quantitative muscle ultrasound) and visual score (Heckmatt score) of a set of muscles (first dorsal interosseous, flexor digitorum profundus, biceps brachii, vastus lateralis, rectus femoris, tibialis anterior, medial and lateral gastrocnemius) in patients with IBM (n=10) and healthy controls (n=20). Echo intensity was higher in most of the examined muscles (flexor digitorum profundus, biceps brachii, vastus lateralis, rectus femoris, tibialis anterior and medial gastrocnemius) in IBM compared to controls. Muscle ultrasound findings correlate with clinical measures (the higher the muscle echo intensity/Heckmatt score, the lower the MRC score of the explored muscle), thus supporting the use of muscle ultrasound in this rare condition. Muscle ultrasound is an easy to perform, inexpensive and reliable diagnostic tool in IBM.

CONCLUSIONS

Neuromuscular ultrasound is an noninvasive tool that provides useful information complementary to neurophysiological data, offering support in investigating peripheral nervous system diseases. It can provide prognostic information (Study 1), and give valuable insights correlating with clinically assessed disability (Study 2 and Study 3).

The implementation of standardized scanning protocols is of paramount importance in order to improve patient care and support a greater applicability of this technique among neurophysiologists.

SUMMARY

1. INTRODUCTION

In the last years, high-resolution ultrasound study of the Peripheral Nervous System has become established as a complementary method to classical neurophysiological studies in neurophysiology laboratories. This technique has a wide range of possible applications and its valuable diagnostic potential is reshaping the way we look at peripheral nervous system diseases (Walker et al., 2018). Yet, there are several obstacles to overcome.

First of all, the lack of reliable evidences and standard scanning protocols regarding some neuromuscular diseases can limit its application (Gonzalez and Hobson-Webb, 2019). Secondly, a cultural gap needs to be filled, since neurophysiologists are not accustomed to incorporate ultrasonography in their clinical practice and often they are not trained to perform neuromuscular ultrasound.

These limitations need to be addressed to allow for a better integration of neurosonology and classical neurophysiological studies, thus improving the way we diagnose and treat neuromuscular diseases.

1.1 Ultrasound principles

Ultrasonographic techniques are based on the transformation of acoustic waves into images. An electric current passing through a transducer is converted into a beam of ultrasound (piezoelectric effect). This occurs due to the physical properties of certain types of crystals or ceramics that can vibrate at high frequency when subjected to an electric current. Tissues affected by the ultrasonic beam reflect the waves, which are captured by the probe and converted back into electrical signals.

In brightness-mode (B-mode) techniques an image is reconstructed; in these images brightness (echo intensity) is proportional to the intensity of the reflected wave. The greater the acoustic impedance at the tissue interface (a function of tissue density and wave propagation velocity), the greater the brightness of the represented structure. Information collected from different transducers in series enables the production of a two-dimensional virtual anatomical map that closely approximates reality.

For the study of the peripheral nervous system, linear probes with frequencies of 18-6 MHz are used, allowing for high spatial resolution (up to 250-500µm). Curvilinear probes are not commonly used but they find application, in selected cases, in the study of deep nerve structures (cervical nerve roots, sciatic nerve (Gonzalez and Hobson-Webb, 2019).

Color-Doppler imaging also provides information about the direction and velocity of blood flow,

identifying relationships between vascular structures and the peripheral nervous system. A further evolution of this technique (Power Doppler) allows visualization of blood flow not based on direction and velocity parameters, but according to the amplitude of the Doppler frequency, enabling the evaluation of both vascular structures with a more tortuous course and intraneural vascular flow (Kerasnoudis and Tsivgoulis, 2015) (Gonzalez and Hobson-Webb, 2019).

1.2 Nerve Ultrasound

1.2.1 Nerve scanning technique

Following superficial anatomical landmarks corresponding to the course of peripheral nerves, major nerve trunks can be directly identified and followed through their course. Nerves can be visualized in axial and longitudinal sections analysing anatomical relationships with surrounding structures. The brachial plexus can be visualized at the supraclavicular fossa and in the interscalene space, following the individual roots more proximally. Cranial nerves can be studied directly (II, VII, X, XI) or indirectly through ultrasound evaluation of the muscles they innervate (Tawfik et al., 2015; Walker et al., 2018).

Nerves in normal conditions appear as round-shaped structures with a honeycomb-like appearance (reflecting the internal fascicular structure) when observed in cross-section (Figure 1) and they appear as tubular structures with a mixture of parallel hypoechoic and hyperechoic lines in the longitudinal plane. Nerves can be easily recognized from surrounding structures due to their low anisotropy (their appearance does not change significantly if the angle of insonation is altered). In proximity to ligamentous or bony structures, the nerve may appear hypoechoic (Gonzalez and Hobson-Webb, 2019).

Nerve ultrasound examination can reveal quantitative and qualitative alterations. The most widely used and accepted parameter for quantitative evaluation of individual nerves is the Cross-Sectional Area (CSA), which corresponds to the value of the area (measured using the ellipse technique or as 'Area Trace') delimited by the epineurium (hyperechoic rim). Similarly, the CSA of individual fascicles within the nerve can be measured in specific pathological conditions. Intranerve CSA variability (maximal CSA/minimal CSA for each nerve) and internerve CSA variability (maximal intranerve CSA variability/ minimal intranerve CSA variability, for each patient) can identify different ultrasound patterns in immune-related neuropathies (Padua et al., 2012).

Proper positioning of the ultrasound probe is essential to obtain reliable and comparable measurements. The transducer is held perpendicular to the nerve to ensure the most accurate view and the best resolution. If the transducer is not perpendicular to the nerve, the CSA can be overestimated. During the examination it is also mandatory not to apply too much pressure, this could change the shape, size and echogenicity of the structure of interest. For this reason using a generous amounts of ultrasound gel is recommended.

Qualitatively, it is possible to inspect the nerve, highlighting focal alterations of the normal fascicular structure and echogenicity, as well as vascularization and nerve mobility. Evaluation through dynamic tests is particularly useful in entrapment and traumatic neuropathies (i.e. ulnar nerve entrapment at the elbow) (Omejec and Podnar, 2016). Additionally, the study of the muscles innervated by a specific nerve may show atrophy and hyperechogenicity in case of denervation (Walker, 2017; Winter et al., 2021).

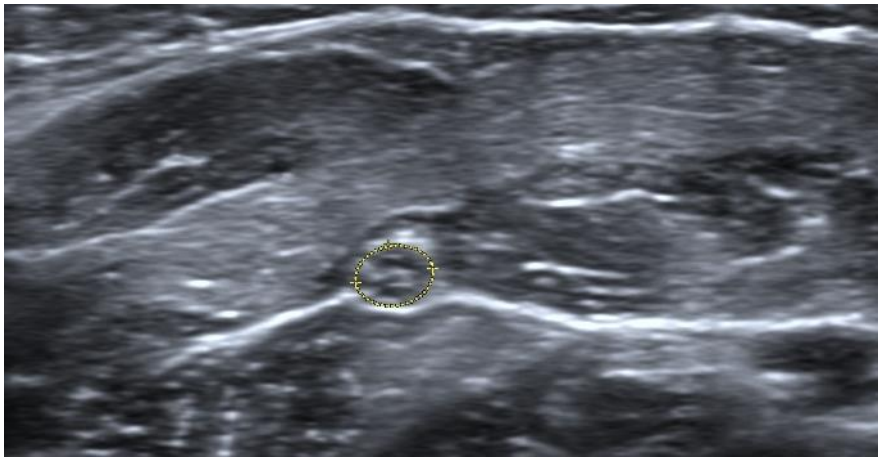

Figure 1. Normal appearance of the median nerve at forearm.

1.2.2 Nerve ultrasound in Neuropathies

The first nerve ultrasound studies focused on compressive neuropathies. In carpal tunnel syndrome and in entrapments of the ulnar nerve at the elbow, ultrasound examination can show an increased CSA of the nerve at the entrapment site and an alteration of the echogenicity with loss of normal structural architecture (Figure 2) (Hobson-Webb and Padua, 2009).

In carpal tunnel syndrome the wrist-to-forearm ratio of median nerve CSA was also introduced, this

measure allows patients to serve as their own control and mitigate the possible variability of measurements between laboratories due to different ultrasound equipment, population and ultrasound settings (Hobson-Webb and Padua, 2009) (Grönfors et al., 2023).

In the study of the ulnar nerve several compression sites can be detected. Proximal compression can occur at the arcade of Struthers, a fibrous band extending from the medial head of the triceps to the intermuscular septum (De Ruiter et al., 2020). Occasionally, an anomalous anconeus epitrochlearis muscle, positioned over the ulnar nerve and extending between the olecranon and medial epicondyle, may serve as a compression source in this area. The ulnar nerve can be also compressed at the cubital tunnel, defined by the medial collateral ligament and the Osborne ligament (Becciolini et al., 2024).

In traumatic nerve lesions, nerve ultrasound proved to be particularly useful, it offers a more comprehensive diagnosis compared to relying solely on neurophysiological studies (Figure 3). In fact, it allows to observe the presence of anomalous structures, dislocation following dynamic nerve maneuvers and alterations in the vascularization that can contribute to neuro-peripheral damage. Anatomical details are frequently essential for determining the most suitable therapeutic approaches and can help deciding the appropriate surgical planning (Padua et al., 2013).

Another significant field of application is represented by inflammatory neuropathies. In these pathological conditions, ultrasound examination shows an increase in nerve CSA associated with focal enlargements and alteration of the fascicular structure. In particular, in Chronic Inflammatory Demyelinating Neuropathies (CIDP) the most characteristic feature is an enlargement mainly of proximal nerve segments in arm and spinal nerve roots; in this setting nerve ultrasound constitutes a valuable supplementary diagnostic method and a potential tool for monitoring the effectiveness of pharmacological treatments (Fisse et al., 2019; Goedee et al., 2017; Merola et al., 2016; Van den Bergh et al., 2021; Zaidman and Pestronk, 2014). In acute inflammatory neuropathies, multidistrict ultrasound involvement patterns with diffuse enlargement of peripheral nerve trunks have been described (Grimm et al., 2014a, 2019).

Genetic neuropathies can exhibit highly suggestive ultrasound patterns, as observed in CMT1a, where a widespread increase in CSA of all nerves with hypoechoic fascicles can be observed (Zanette et al., 2018)

Axonal neuropathies, typically are not associated with significant nerve ultrasound alterations, aside from specific conditions (Grimm et al., 2014b; Leonardi et al., 2022; Salvalaggio et al., 2020).

Only few studies focused on the role of nerve ultrasound in cranial neuropathies (Tawfik et al., 2015).

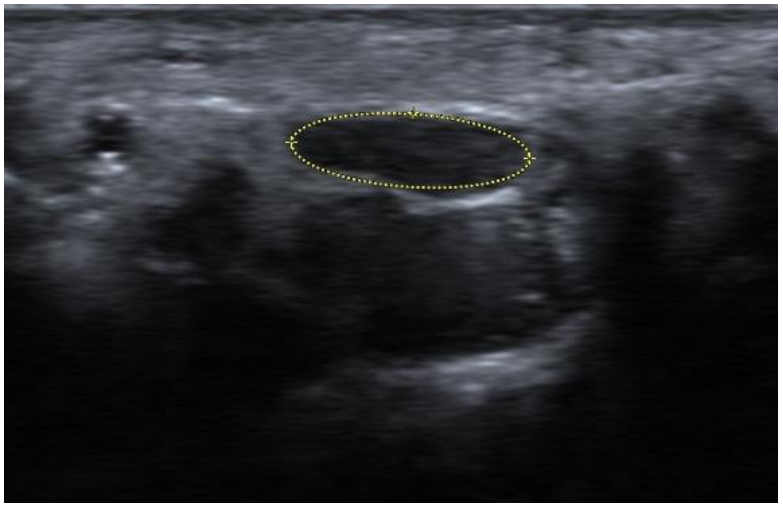

Figure 2. Enlarged median nerve in a patient with carpal tunnel syndrome.

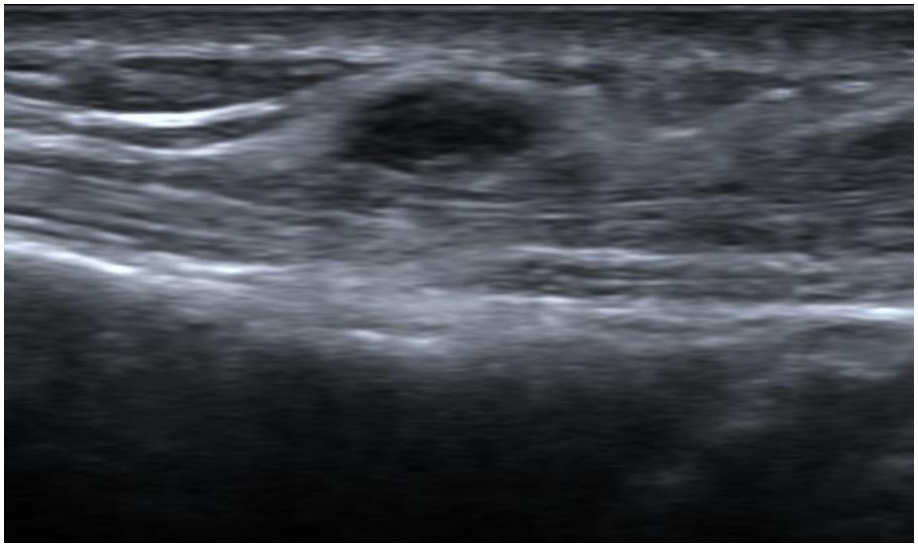

Figure 3. Superficial radial nerve neuroma after a forearm trauma.

1.3 Muscular Ultrasound

1.3.1 Muscle scanning technique

The distinguishing ultrasound appearance of muscle is related to its microscopic anatomy. In healthy

subjects, muscle fibres are hypoechoic, and fibro-adipose and perimysial connective tissues are hyperechoic.

In the transverse plane this results in the typical appearance of muscles: the “starry night appearance”, with black looking muscle fibres interspersed with white fascial structures (Figure 4). In longitudinal images, the muscle fibre direction and pennation angles can be visualized (Wijntjes and Van Alfen, 2021).

There is a wide variation in muscle echogenicity depending on the patient's age and sex. In neonates, the muscle is more hypoechoic and has fewer myofascial planes; in childhood, echogenicity remains stable, and in adulthood, it increases due to fat turnover and fibrosis, more rapidly in advanced age. Muscles in boys are slightly more hyperechoic than those in girls, and the difference persists throughout adulthood. Visual (qualitative) and quantitatively evaluated echogenicity are the most commonly used clinical muscle ultrasound parameter (Heckmatt et al., 1982) (Walker, 2017) (Wijntjes et al., 2022).

Ultrasound can also evaluate other muscle tissue properties such as muscle atrophy, muscle vascularization and elasticity. A unique feature of ultrasound is its ability to capture dynamic images, which can be used to localize a specific muscle and confirm its contraction.

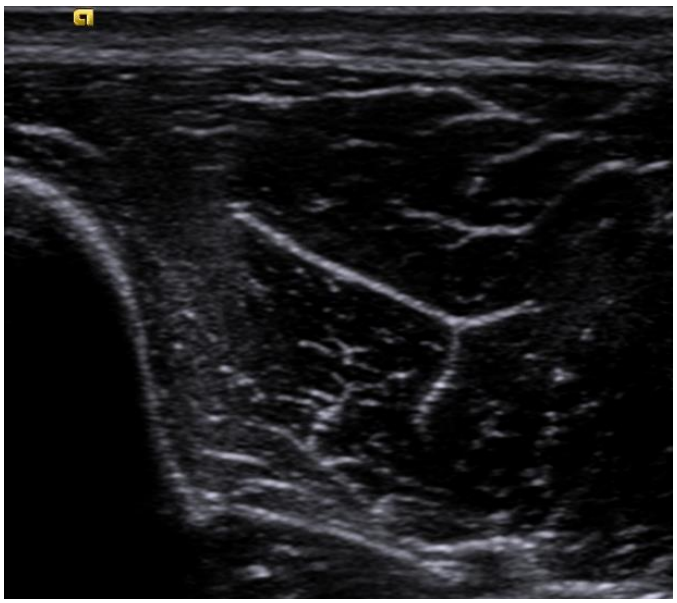

Figure 4. Normal appearance of the tibialis anterior muscle.

1.3.2 Muscle ultrasound in Myopathies

Any disorder disrupting muscular architecture, causing oedema, fibrosis, necrosis, inflammation, or tissue replacement, will result in a change in the ultrasound image. These changes almost invariably lead to increased echogenicity due to an increase in the number and diversity of reflecting points on the muscle tissue surface (Figure 5). Such changes are often accompanied by atrophy. Atrophy is associated with reduction in muscle volume and a relative increase in subcutaneous tissue. In the context of myopathies, muscular ultrasound can help define the pattern of muscle involvement and recognize the most involved sites (Leeuwenberg et al., 2020).

The rapid accessibility and high feasibility in follow-up studies have favoured the use of neuromuscular ultrasound even in muscular dystrophies and inflammatory myopathies. Adipose turnover and fibrosis observed in muscular dystrophies result in greater tissue heterogeneity within the muscle, leading to hyper-echogenicity on ultrasound. Additionally, there is a progressive attenuation of the underlying bone signal. Atrophy may result in decreased muscle thickness and increased subcutaneous tissue depth. In inflammatory myopathies, unlike dystrophies where bone structures are obscured, deep bone structures can be visualized despite a significantly increased echogenicity (Pillen et al., 2016).

Both qualitative and quantitative evaluations can be performed to measure the degree of muscle pathology. Heckmatt et al. introduced a four-point assessment scale for the visual assessment of neuromuscular images (1 normal, 2 increased muscle echo intensity with distinct bone echo, 3 marked increased muscle echo intensity with a reduced bone echo, 4 very strong muscle echo and complete loss of bone echo) (Heckmatt et al., 1982). Some studies have shown that the Heckmatt scale has moderate to good diagnostic values for detecting muscle alterations. In contrast, quantitative muscle ultrasound measures the mean value of the grayscale of a region of interest (ROI) in the muscle; this value can be compared with a reference value. Compared to the qualitative classification of Heckmatt, this analysis improves diagnostic value from 70% to 90% (Wijntjes et al., 2022).

Figure 5. Increased ecogenicity in the vastus lateralis muscle of a patient diagnosed with Inclusion Body Myositis.

2. AIM OF THE PROJECT

This study series aims primarily to define the utility of neuromuscular ultrasound in specific neuromuscular diseases; defining its feasibility and field of application. Secondly, it aims to investigate the association between clinical, neurophysiological and neurosonological data.

Our findings may finally improve the way we use neuromuscular ultrasound in clinical practice.

3. SUMMARY OF THE MAIN FINDINGS

Study 1. Predicting value for incomplete recovery in Bell's palsy of facial nerve

ultrasound versus nerve conduction study.

This longitudinal study aimed at assessing the predictive value of facial nerve ultrasound in patients with Bell's palsy. To do so, we have investigated facial nerve diameter as assessed with ultrasound at three different time points and verified if its predictive value for incomplete facial muscle recovery is higher than that of the facial nerve conduction study. In the first days after Bell's palsy onset, the diameter of the affected facial nerve is increased compared with the normal side. The negative predictive value of a facial nerve diameter asymmetry of 25 % was relatively high (i.e., 94.73 %); thus we may speculate that an asymmetry lower than this threshold might be sensitive in detecting patients with a high probability of complete recovery. However, facial nerve ultrasound examination has a poorer prognostic value than facial nerve conduction study in patients with Bell's palsy.

Study 2. Nerve Ultrasound in Friedreich's Ataxia: enlarged nerves as a biomarker of disease severity.

While nerve conduction studies can effectively identify sensory neuropathy in Friedreich's ataxia, sensory nerve action potentials are often significantly reduced or completely absent. This occurrence suggests a floor effect, thus limiting the ability of nerve conduction study to measure disease severity or treatment effects, thus diminishing its potential as a biomarker in patients with Friedreich's ataxia. In this study, our aim was to investigate whether nerve ultrasound might serve as a potential biomarker in patients with Friedreich's ataxia.

Ten patients diagnosed with Friedreich's Ataxia underwent an extensive clinical evaluation (SARA, FARS, mFARS, INCAT, ADL 0-36, IADL). Furthermore, they underwent nerve conduction study and nerve ultrasound examination. The quantitative assessment of nerve cross-sectional area, performed at 24 nerve sites, was compared to data collected from 20 healthy volunteers. All the patients had a severe sensory axonal neuropathy. Nerve ultrasound showed a significant enlargement of median and ulnar nerves at the axilla and arm. The cumulative count of affected nerve sites was directly associated with clinical disability.

Study 2 showed that nerve ultrasound can offer valuable insights in cases where nerve conduction studies yield limited information and that nerve ultrasound is a potential biomarker of disease severity in Friedreich's Ataxia.

Study 3. Muscle ultrasound in Inclusion Body Myositis.

Study 3 aimed at evaluating the echo intensity (quantitative muscle ultrasound) and visual score (Heckmatt scale) of a set of muscles (first dorsal interosseous, flexor digitorum profundus, biceps brachii, vastus lateralis, rectus femoris, tibialis anterior, medial and lateral gastrocnemius) in patients with IBM (n=10) compared with healthy controls (n=20). Echo intensity was higher in most of the examined muscles (flexor digitorum profundus, biceps brachii, vastus lateralis, rectus femoris, tibialis anterior and medial gastrocnemius) in IBM compared to controls. In IBM patients muscle ultrasound findings correlate with clinical measures (the higher the muscle echo intensity/Heckmatt score the lower the MRC score of the explored muscle), thus supporting the use of muscle ultrasound as a disease biomarker in this rare condition.

Muscle ultrasound is a easy to perform, inexpensive, radiation free diagnostic tool in IBM.

4. CONCLUSIONS

Neuromuscular ultrasound is a noninvasive, easy to perform tool that provides useful information complementary to neurophysiological data, offering support in investigating peripheral nervous system diseases. In specific conditions (i.e. Friedreich's ataxia, IBM) ultrasound findings correlate with clinical scales thus possibly being applied as biomarker of disease severity and progression.

In all the examined conditions we gathered evidence supporting the implementation of standardized scanning protocols; these results are of paramount importance in order to improve patient care and support a greater applicability of this technique among neurophysiologists.

References

Becciolini, M., Pivec, C., Raspanti, A., Riegler, G., 2024. Ultrasound of the Ulnar Nerve: A Pictorial Review: Part 1: Normal Ultrasound Findings. J. Ultrasound Med. 43, 171–188. https://doi.org/10.1002/jum.16350

De Ruiter, G.C.W., De Jonge, J.G.H., Vlak, M.H.M., Van Loon-Felter, A.E., 2020. Ulnar Neuropathy Caused by Muscular Arcade of Struthers. World Neurosurg. 142, 128–130. https://doi.org/10.1016/j.wneu.2020.06.179

Fisse, A.L., Pitarokoili, K., Trampe, N., Motte, J., Kerasnoudis, A., Gold, R., Yoon, M.-S., 2019. Clinical, Sonographic, and Electrophysiologic Longitudinal Features of Chronic Inflammatory

Demyelinating Polyneuropathy: Long-Term Clinical, Sonographic, and Electrophysiologic Characteristics of CIDP. J. Neuroimaging 29, 223–232. https://doi.org/10.1111/jon.12579

Goedee, H.S., van der Pol, W.L., van Asseldonk, J.-T.H., Franssen, H., Notermans, N.C., Vrancken, A.J.F.E., van Es, M.A., Nikolakopoulos, S., Visser, L.H., van den Berg, L.H., 2017. Diagnostic value of sonography in treatment-naive chronic inflammatory neuropathies. Neurology 88, 143–151. https://doi.org/10.1212/WNL.0000000000003483

Gonzalez, N.L., Hobson-Webb, L.D., 2019. Neuromuscular ultrasound in clinical practice: A review. Clin. Neurophysiol. Pract. 4, 148–163. https://doi.org/10.1016/j.cnp.2019.04.006

Grimm, A., Décard, B.F., Axer, H., 2014a. Ultrasonography of the peripheral nervous system in the early stage of Guillain-Barré syndrome: Grimm et al. J. Peripher. Nerv. Syst. 19, 234–241. https://doi.org/10.1111/jns.12091

Grimm, A., Heiling, B., Schumacher, U., Witte, O.W., Axer, H., 2014b. Ultrasound differentiation of axonal and demyelinating neuropathies: Ultrasound in Polyneuropathy. Muscle Nerve 50, 976–983. https://doi.org/10.1002/mus.24238

Grimm, A., Oertl, H., Auffenberg, E., Schubert, V., Ruschil, C., Axer, H., Winter, N., 2019. Differentiation Between Guillain–Barré Syndrome and Acute-Onset Chronic Inflammatory Demyelinating Polyradiculoneuritis—a Prospective Follow-up Study Using Ultrasound and Neurophysiological Measurements. Neurotherapeutics 16, 838–847. https://doi.org/10.1007/s13311-019-00716-5

Grönfors, H., Himanen, S.-L., Martikkala, L., Kallio, M., Mäkelä, K., 2023. Median nerve ultrasound cross sectional area and wrist-to-forearm ratio in relation to carpal tunnel syndrome related axonal damage and patient age. Clin. Neurophysiol. Pract. 8, 81–87. https://doi.org/10.1016/j.cnp.2023.02.003

Heckmatt, J.Z., Leeman, S., Dubowitz, V., 1982. Ultrasound imaging in the diagnosis of muscle disease. J. Pediatr. 101, 656–660. https://doi.org/10.1016/S0022-3476(82)80286-2

Hobson-Webb, L.D., Padua, L., 2009. Median nerve ultrasonography in carpal tunnel syndrome: Findings from two laboratories. Muscle Nerve 40, 94–97. https://doi.org/10.1002/mus.21286

Kerasnoudis, A., Tsivgoulis, G., 2015. Nerve Ultrasound in Peripheral Neuropathies: A Review: Nerve Ultrasound in Peripheral Neuropathies. J. Neuroimaging 25, 528–538. https://doi.org/10.1111/jon.12261

Leeuwenberg, K.E., Alfen, N., Christopher-Stine, L., Paik, J.J., Tiniakou, E., Mecoli, C., Doorduin, J., Saris, C.G.J., Albayda, J., 2020. Ultrasound can differentiate inclusion body myositis from disease mimics. Muscle Nerve 61, 783–788. https://doi.org/10.1002/mus.26875

Leonardi, L., Di Pietro, G., Di Pasquale, A., Vanoli, F., Fionda, L., Garibaldi, M., Galosi, E., Alfieri, G., Lauletta, A., Morino, S., Salvetti, M., Truini, A., Antonini, G., 2022. High-resolution ultrasound of peripheral nerves in late-onset hereditary transthyretin amyloidosis with polyneuropathy:

similarities and differences with CIDP. Neurol. Sci. 43, 3387–3394. https://doi.org/10.1007/s10072-021-05749-3

Merola, A., Rosso, M., Romagnolo, A., Peci, E., Cocito, D., 2016. Peripheral Nerve Ultrasonography in Chronic Inflammatory Demyelinating Polyradiculoneuropathy and Multifocal Motor Neuropathy: Correlations with Clinical and Neurophysiological Data. Neurol. Res. Int. 2016, 1–9. https://doi.org/10.1155/2016/9478593

Omejec, G., Podnar, S., 2016. Does ulnar nerve dislocation at the elbow cause neuropathy?: Ulnar Nerve Dislocation. Muscle Nerve 53, 255–259. https://doi.org/10.1002/mus.24786

Padua, L., Di Pasquale, A., Liotta, G., Granata, G., Pazzaglia, C., Erra, C., Briani, C., Coraci, D., De Franco, P., Antonini, G., Martinoli, C., 2013. Ultrasound as a useful tool in the diagnosis and management of traumatic nerve lesions. Clin. Neurophysiol. 124, 1237–1243. https://doi.org/10.1016/j.clinph.2012.10.024

Padua, L., Martinoli, C., Pazzaglia, C., Lucchetta, M., Granata, G., Erra, C., Briani, C., 2012. Intra- and internerve cross-sectional area variability: New ultrasound measures: Ultrasound Neuropathy Measures. Muscle Nerve 45, 730–733. https://doi.org/10.1002/mus.23252

Pillen, S., Boon, A., Van Alfen, N., 2016. Muscle ultrasound, in: Handbook of Clinical Neurology. Elsevier, pp. 843–853. https://doi.org/10.1016/B978-0-444-53486-6.00042-9

Salvalaggio, A., Coraci, D., Cacciavillani, M., Obici, L., Mazzeo, A., Luigetti, M., Pastorelli, F., Grandis, M., Cavallaro, T., Bisogni, G., Lozza, A., Gemelli, C., Gentile, L., Ermani, M., Fabrizi, G.M., Plasmati, R., Campagnolo, M., Castellani, F., Gasparotti, R., Martinoli, C., Padua, L., Briani, C., 2020. Nerve ultrasound in hereditary transthyretin amyloidosis: red flags and possible progression biomarkers. J. Neurol. https://doi.org/10.1007/s00415-020-10127-8

Tawfik, E.A., Walker, F.O., Cartwright, M.S., 2015. Neuromuscular Ultrasound of Cranial Nerves. J. Clin. Neurol. 11, 109. https://doi.org/10.3988/jcn.2015.11.2.109

Van den Bergh, P.Y.K., Doorn, P.A., Hadden, R.D.M., Avau, B., Vankrunkelsven, P., Allen, J.A., Attarian, S., Blomkwist-Markens, P.H., Cornblath, D.R., Eftimov, F., Goedee, H.S., Harbo, T., Kuwabara, S., Lewis, R.A., Lunn, M.P., Nobile-Orazio, E., Querol, L., Rajabally, Y.A., Sommer, C., Topaloglu, H.A., 2021. European Academy of Neurology/Peripheral Nerve Society guideline on diagnosis and treatment of chronic inflammatory demyelinating polyradiculoneuropathy: Report of a joint Task Force—Second revision. Eur. J. Neurol. 28, 3556–3583. https://doi.org/10.1111/ene.14959

Walker, F.O., 2017. Ultrasonography in Peripheral Nervous System Diagnosis: Contin. Lifelong Learn. Neurol. 23, 1276–1294. https://doi.org/10.1212/CON.0000000000000522

Walker, F.O., Cartwright, M.S., Alter, K.E., Visser, L.H., Hobson-Webb, L.D., Padua, L., Strakowski, J.A., Preston, D.C., Boon, A.J., Axer, H., van Alfen, N., Tawfik, E.A., Wilder-Smith, E., Yoon, J.S., Kim, B.-J., Breiner, A., Bland, J.D.P., Grimm, A., Zaidman, C.M., 2018. Indications for

neuromuscular ultrasound: Expert opinion and review of the literature. Clin. Neurophysiol. 129, 2658–2679. https://doi.org/10.1016/j.clinph.2018.09.013

Wijntjes, J., Van Alfen, N., 2021. Muscle ultrasound: Present state and future opportunities. Muscle Nerve 63, 455–466. https://doi.org/10.1002/mus.27081

Wijntjes, J., Van Der Hoeven, J., Saris, C.G.J., Doorduin, J., Van Alfen, N., 2022. Visual versus quantitative analysis of muscle ultrasound in neuromuscular disease. Muscle Nerve 66, 253–261. https://doi.org/10.1002/mus.27669

Winter, N., Vittore, D., Gess, B., Schulz, J.B., Grimm, A., Dohrn, M.F., 2021. New Keys to Early Diagnosis: Muscle Echogenicity, Nerve Ultrasound Patterns, Electrodiagnostic, and Clinical Parameters in 150 Patients with Hereditary Polyneuropathies. Neurotherapeutics 18, 2425–2435. https://doi.org/10.1007/s13311-021-01141-3

Zaidman, C.M., Pestronk, A., 2014. Nerve size in chronic inflammatory demyelinating neuropathy varies with disease activity and therapy response over time: A retrospective ultrasound study: Nerve Size in CIDP. Muscle Nerve 50, 733–738. https://doi.org/10.1002/mus.24227

Zanette, G., Fabrizi, G.M., Taioli, F., Lauriola, M.F., Badari, A., Ferrarini, M., Cavallaro, T., Tamburin, S., 2018. Nerve ultrasound findings differentiate Charcot-Marie-Tooth disease (CMT) 1A from other demyelinating CMTs. Clin. Neurophysiol. 129, 2259–2267. https://doi.org/10.1016/j.clinph.2018.08.016

STUDY 1.

Predicting value for incomplete recovery in Bell's palsy of facial nerve ultrasound versus nerve conduction study.

Clin Neurophysiol. 2024 Feb:158:35-42. doi: 10.1016/j.clinph.2023.11.020. Epub 2023 Dec 4

Abstract

Objective: This longitudinal study aims at assessing the predictive value of facial nerve high-resolution ultrasound (HRUS) for incomplete clinical recovery in patients with Bell's palsy, the most common facial nerve disease.

Methods: We prospectively enrolled 34 consecutive patients with Bell's palsy. All patients underwent neurophysiological testing (including facial nerve conduction study) and HRUS evaluations 10-15 days (T1), one month (T2), and three months (T3) after the onset of Bell's palsy. Patients who did not experience complete recovery within three months were also evaluated after six months (T4). We have then compared the accuracy of HRUS with that of the facial nerve conduction study in predicting incomplete clinical recovery at three and six months.

Results: At T1, the facial nerve diameter, as assessed with HRUS, was larger on the affected side than on the normal side, particularly in patients with incomplete recovery at T2, T3 and T4. ROC curve analysis, however, showed that the facial nerve diameter at T1 had a lower predictive value than the facial nerve conduction study for an incomplete clinical recovery at three (T3) and six (T4) months. Still, the facial nerve diameter asymmetry, as assessed with HRUS, had a relatively high negative predictive value (thus indicating a strong association between normal HRUS examination and a good prognosis).

Conclusions: Although HRUS shows abnormally increased facial nerve diameter in patients in the acute phase of Bell's palsy, the predictive value of this technique for incomplete clinical recovery at three and six months is lower than that of the nerve conduction study.

Significance: Nerve ultrasound has a low predictive value for incomplete clinical recovery in patients with Bell's Palsy.

Keywords: Bell's palsy; Facial nerve conduction study; High-resolution nerve ultrasound.

1.Introduction

Bell's palsy is the most common cause of acute peripheral facial palsy (Eviston et al., 2015). The clinical picture is dominated by a rapid-onset, unilateral facial weakness associated with a wide spectrum of signs and symptoms due to the variable degree of facial nerve involvement. Most patients recover within a few months, while up to a third have a residual functional deficit with facial muscle weakness or synkinesis (De Seta et al., 2014; Yoo et al., 2020). Conventional neurophysiological testing is informative at all stages of Bell's palsy (Valls-Solé, 2007). A preserved amplitude of the compound muscle action potential in the early phase of facial nerve palsy is likely the most informative test for determining the prognosis (Gantz et al., 1999). Beyond 20 days after onset, needle EMG recording brings an approximate measure of the intensity of denervation. A large retrospective study showed that spontaneous fibrillation at needle electromyography investigation predicts unfavourable outcomes with an accuracy of 80.8 % (Sittel and Stennert, 2001). Although neurophysiological tests are widely used for the assessment and prognostic evaluation of Bell's palsy (Valls-Solé, 2007), they cannot provide direct information on the structural damage of the facial nerve caused by oedema and inflammation (Kimura et al., 1976; Ozgur et al., 2010; Tawfik et al., 2015a; Valls-Solé, 2007). High-resolution nerve ultrasound (HRUS) has increasingly been used to investigate peripheral nervous system conditions. HRUS detects nerve oedema and inflammation and has been proven helpful for diagnosing and monitoring entrapment and inflammatory neuropathies (Van den Bergh et al., 2021; Walker et al., 2018; Hsueh et al., 2020). Facial nerve HRUS may provide evidence of nerve oedema spreading distally from the site of facial nerve damage in Bell's palsy (i.e., the intratemporal portion), thus possibly improving how we diagnose this common condition. Nevertheless, only a few studies have investigated whether HRUS might provide clinically useful information in patients with Bell's palsy. Additionally, these studies provided contradicting findings on the diagnostic usefulness of facial nerve HRUS, probably due to different methodological approaches (Baek et al., 2020; Li et al., 2016; Lo et al., 2010; Tawfik et al., 2015b). Accordingly, the diagnostic value of this technique in patients with Bell's palsy is still unclear. Understanding more about the diagnostic value of facial nerve HRUS and whether this technique is more informative than facial nerve conduction study for predicting recovery in patients with Bell's palsy might improve the clinical management of this common peripheral nervous system disease. This longitudinal study aims

at assessing the predictive value of facial nerve HRUS in patients with Bell's palsy. To do so, we have investigated facial nerve diameter as assessed with HRUS at three different time points and verified if its predictive value for incomplete facial muscle recovery is higher than that of the facial nerve conduction study.

2. Methods

2.1. Study cohort and design

In this longitudinal study, we prospectively screened patients with a definite diagnosis of Bell's palsy, who were referred to the emergency department of our hospital within 48 hours of the onset of Bell's palsy. Exclusion criteria were age under 18 years, bilateral facial palsy, previous cranial neuropathies, a known history of central or peripheral nervous system disease, pregnancy, and signs and/or symptoms of Varicella Zoster Virus infection. At the time of diagnosis, as part of the emergency assessment of acute facial weakness, all the patients underwent a complete neurological and otolaryngological assessment with microscopic examination to magnify both ears' external canal and the tympanic membrane. All patients also underwent a head CT scan to identify possible structural lesions (e.g., stroke or tumours); clinical and CT examinations showed no abnormalities. All the patients diagnosed with Bell's palsy were started on a standardized oral pharmacological treatment with prednisone 1 mg/Kg for 10 days. In all patients included in the study, treatment was started within 24 hours (IQR 23–42) from symptoms onset. All patients underwent clinical examination, neurophysiological testing, and facial nerve HRUS at three distinct time points: T1 corresponding to 10–15 days from symptoms onset, T2 corresponding to one month (±2 days), T3 corresponding to three months (±2 days) after Bell's palsy onset; the patients who did not experience complete recovery within three months also underwent clinical examination after six months (T4). At T1, all patients had completed the corticosteroid treatment (Supplementary Table 1). All the patients without a complete recovery within one month from the onset of the symptoms underwent a gadolinium enhancement brain and maxillofacial MRI (1.5 T) focused on the facial nerve path to rule out other possible alternative causes of peripheral facial nerve palsy. All data were collected in a structured form using standardized protocols by staff members (clinical examination: AT, PM, CDE; neurophysiological testing: GDS, EG, CL; HRUS: GDP, PF). The primary outcomes of interest included the amplitude of the compound muscle action potential of the facial nerve as assessed with

neurophysiological testing and the diameter of the facial nerve as assessed with the HRUS. The study was approved by the local institutional review board. Written informed consent to participate was obtained from all participants.

2.2. Clinical evaluation

We collected demographic and clinical information, including sex, age, and comorbidities at time points T1, T2, T3, T4. At each point, facial muscle deficit was assessed with the House-Brackmann Facial Grading System (HB) (House and Brackmann, 1985). During the clinical examination, we collected detailed data regarding Bell's palsy-associated symptoms (auricular and retro auricular pain, dysgeusia, hyper lacrimation, dry eye, hyperacusis, and aural fullness).

2.3. Neurophysiological and nerve ultrasound investigation

At time points T1, T2, T3, the patients underwent a complete neurophysiological evaluation. Facial nerve CMAP was recorded bilaterally by stimulating the nerve anterior to the mastoid process (stimulus duration: 0.2 ms; stimulation intensity: 15–50 mA; filters: 20 Hz-2 kHz), with the recording electrodes placed over the nasalis muscle. The percentage of asymmetry of the CMAP amplitude compared to the control side was calculated as: (CMAP amplitude affected - CMAP amplitude control side)/CMAP amplitude control side*100. The blink reflex was recorded bilaterally, stimulating the supraorbital nerve, with surface recording electrodes over the inferior orbicularis oculi muscles (stimulus duration: 0.1 ms; stimulation intensity: 15–40 mA; filters: 20 Hz-2 kHz). Blink reflex responses were defined as presence/absence of the R1 blink reflex response. Needle electromyography (EMG) was performed on the orbicularis oris and orbicularis oculi muscles on the affected side. We collected EMG data regarding presence/absence of denervation and electromyographic voluntary activity (qualitative pattern evaluation with full voluntary force, scored as 0: no activity, 1: discrete recruitment, 2: reduced recruitment, 3: normal recruitment). In the same session dedicated to clinical examination and neurophysiological testing (T1, T2, T3), patients underwent facial nerve HRUS examination with an 18 MHz linear array transducer (Siemens S2000, Virtual Touch IQ). A standardized scanning protocol was applied to ensure the reproducibility of the test (the settings were kept constant during all examinations, depth = 3 cm). With the patient lying supine and the probe placed just under the ear lobule, two operators (GDP, PF) blinded to the

neurophysiological data assessed the facial nerve bilaterally. The nerve was examined along its longitudinal course inside the parotid gland after it emerges from the stylomastoid foramen, where it appears as a thin tubular structure, dividing the superficial and the deep lobe of the gland. The probe was kept perpendicular to the skin with minimal pressure to ensure precise measurements. The facial nerve diameter was measured at the point of maximum enlargement within the epineural rim. The average facial nerve diameter calculated by the two operators was then used as an outcome variable. The percentage of asymmetry of the diameter compared to the control side was calculated as (diameter affected-diameter control side)/diameter control side*100.

2.4. Statistics

The normality assumption was assessed with the KolmogorovSmirnov test. We used the Cronbach's alpha test to establish an agreement for facial nerve diameter assessment between the two operators (GDP, PF). We used the Mann-Whitney test to assess differences between independent groups, Wilcoxon test was used for paired values. Two-way repeated measures analysis of variance (ANOVA) was used to assess facial nerve diameter as assessed with HRUS and CMAP amplitude with the variables time (T1, T2, T3) and side (affected, control). A post hoc multiple comparisons test with Sidak correction was then performed. Categorical variables between independent groups were compared with the chi-squared test and Fisher's exact test as appropriate. A p-value of 0.05 was considered statistically significant. We used the Receiver Operating Characteristic (ROC) analysis to assess the discriminative ability for incomplete recovery at three and six months from the Bell's palsy onset for nerve conduction study and HRUS data collected at T1. The Youden index assessed the best diagnostic value for nerve conduction study and HRUS; relative sensitivity, specificity, positive predictive value (PPV), and negative predictive value (NPV) were then estimated. Statistical analyses were performed using Prism 9.4 (GraphPad, CA, USA).

3. Results

We consecutively screened 39 patients and excluded five (two due to Varicella Zoster Virus infection and three due to concomitant diabetic neuropathy). We therefore enrolled 34 patients (age 55 years, IQR 40–65; 16 men) with a definite diagnosis of Bell's Palsy (Supplementary Table 1). Three patients were lost at follow-up after the first evaluation (Table 1). The Cronbach's alpha test showed a good

inter-operator agreement for facial nerve diameter measurements with HRUS (T1 a = 0.86, T2 a = 0.89, T3 a = 0.9). At T1, the facial nerve diameter was larger ($p = 0.001$), (Fig. 1) and the CMAP amplitude was lower ($p < 0.0001$) in the affected side than in the normal side. At T1, 24 patients had a preserved R1 blink reflex. The two-way repeated measure ANOVA for the facial nerve diameter, as assessed with HRUS, showed a significant interaction between time (T1, T2, T3) and side (affected, control side) ($F(2, 120) = 3.088$, $p < 0.05$), (Fig. 2). Post hoc analysis showed a significant difference between facial nerve diameter at T1 and T3 on the affected side ($p = 0.005$, Fig. 2), indicating a progressive reduction in the facial nerve diameter on the affected side. The two-way repeated measure ANOVA for the facial nerve CMAP amplitude showed a significant interaction between time (T1, T2, T3) and side (affected, control side) ($F(2, 120) = 11.83$, $p < 0.001$). Post hoc analysis showed a significant difference between facial nerve CMAP amplitude at T1 and T3 on the affected side ($p < 0.001$), indicating a progressive increase in the facial nerve CMAP amplitude on the affected side. One month after symptoms onset (T2) seven patients of the 34 patients enrolled had a complete clinical recovery (i.e., HB = 1). All these seven patients had a preserved R1 blink reflex at T1 and a significantly lower facial nerve diameter at T1, compared to patients with incomplete recovery (i.e., HB > 1), ($p = 0.023$), (Table 2). At three (T3) and six months (T4) after Bell's palsy onset, twenty and twenty-four patients of the 34 enrolled had a complete clinical recovery (i.e., HB = 1). All these patients had a larger facial nerve CMAP and a smaller facial nerve diameter at T1 when compared with patients with incomplete recovery (i.e., HB > 1), ($p < 0.05$), (Tables 3 and 4). The ROC curve analysis showed that the asymmetry of the CMAP amplitude between the affected and normal side at T1 had a better performance than the facial nerve diameter asymmetry as assessed with HRUS in predicting patients with incomplete recovery (i.e., HB > 1) at three (AUC = 0.88 vs AUC = 0.76, PPV = 88.88 % vs PPV = 58.33 %) and six (AUC = 0.91 vs AUC = 0.79, PPV = 66.66 % vs PPV = 50 %) months (Fig. 3), (Table 5). The optimal trade-off value between sensitivity and specificity corresponded to a facial nerve diameter asymmetry of 25 % (an increase in the diameter on the affected side higher than the 25 % of the control side) and a CMAP amplitude asymmetry of 65 % (a decrease in the CMAP amplitude on the affected side more than the 65 % of the control side).

4. Discussion

Our longitudinal study found that although the HRUS showed an increased facial nerve diameter

during the first days of Bell's palsy onset, the predictive value for the incomplete recovery of this HRUS variable is lower than that of CMAP amplitude. Predicting facial muscle recovery in patients with Bell's palsy relies on clinical and neurophysiological findings (Yoo et al., 2020). In particular, the predictive value of CMAP amplitude asymmetry between the affected and normal side is an established approach for estimating axonal loss and providing prognostic information. Previous observations indicated that a 90 % facial nerve CMAP reduction is associated with incomplete clinical recovery (grade III HB or higher), (Valls-Solé, 2007; Ozgur et al., 2010; Halvorson et al., 1993; Gantz et al., 1999). In our study, we investigated the clinical usefulness of HRUS for predicting clinical recovery in patients with Bell's palsy. Compared with MRI, HRUS is less expensive, easy to perform and allows serial studies of the distal portion of the facial nerve after its emergence at the stylomastoid foramen. The cross-sectional area is the most widely used ultrasound parameter in assessing peripheral nerve conditions. Conversely, in our study, we used the diameter of the facial nerve as the main outcome measure, given that the facial nerve is a tiny nerve in the relatively isoechoic salivary gland tissue. Accordingly, an isolated axial view of the facial nerve is often technically challenging (Tawfik et al., 2015b). We found that in the first days after Bell's palsy onset, the diameter of the affected facial nerve is increased compared with the normal side, a finding in line with previous observations (Tawfik et al., 2015a). Facial nerve swelling may be due to the spreading along the nerve of oedema and inflammation secondary to nerve entrapment in the facial canal (Liston and Kleid, 1989; Michaels, 1990). Remarkably, all the patients who had complete recovery within one month from symptoms onset (i.e., having an HB 1) had a smaller facial nerve diameter at T1 (10–15 days after the Bell's palsy onset) compared with patients with incomplete recovery. Moreover, all these patients had a preserved R1 blink response. A less prominent nerve enlargement associated with a preserved R1 blink reflex response may therefore reflect a negligible axonal loss and inflammation after nerve injury in this subgroup of patients, regardless of the clinically evident severity (as assessed with HB) and the facial CMAP amplitude reduction. The ROC curve analysis showed that the optimal trade-off between sensitivity and specificity for the facial nerve asymmetry assessed with HRUS at T1 corresponded to 25 % (an increase in the diameter on the affected side higher than 25 % of the control side). This threshold, however, had a lower sensitivity and specificity for predicting the incomplete recovery at three (T3) and six (T4) months than the facial nerve CMAP asymmetry. This finding may reflect the different diagnostic characteristics of neurophysiological testing and nerve HRUS (Kerasnoudis et al., 2015). HRUS explores only the distal portion of the facial nerve, while

histopathological studies demonstrated that in patients with Bell's palsy oedema and inflammation affect the nerve mainly in the facial canal of the temporal bone (Michaels, 1990). Nevertheless, the negative predictive value of a facial nerve diameter asymmetry of 25 % was relatively high (i.e., 94.73 %). Accordingly, we may speculate that an asymmetry lower than this threshold might be sensitive in detecting patients with a high probability of complete recovery. Our findings on the predictive value of facial nerve HRUS in patients with Bell's palsy are in line with a previous study that in a relatively small sample of patients with Bell's palsy (Baek et al., 2019) demonstrated that the facial nerve diameter does not correlate with the HB at two months after the onset of Bell's palsy (Baek et al., 2020). Our longitudinal study extends this knowledge and provides previously unreported findings, given that we have now precisely analysed how facial nerve HRUS predicts the recovery in patients with Bell's palsy and provided the sensitivity and specificity of this technique for the incomplete recovery at three and six months after this facial nerve palsy. Although the predictive value of facial nerve HRUS is lower than that of facial nerve conduction study, we believe that it may represent a potentially useful diagnostic tool in the diagnostic pathway of facial palsy. Ultrasound investigation offers a relatively low-cost, easy-to-perform, non-invasive tool for rapidly evaluating the distal portion of the facial nerve. Furthermore, a less prominent nerve enlargement after 10–15 days is associated with a good outcome at one month from disease onset (regardless of clinical and CMAP amplitude impairment).

4.1. Limitations

Admittedly our study has some limitations. Facial nerve HRUS is an operator-dependent procedure, therefore the reproducibility of this technique is still an open issue; this limitation may affect our findings. However, in our study we used a standardized ultrasound protocol to improve the reproducibility of this technique and demonstrated a good inter-rater reliability between the two operators. An additional limitation is that we have excluded patients with concomitant peripheral nervous system conditions (e.g., diabetes). It follows that our findings on the relatively low predictive value of facial nerve HRUS may have a poor validity for the different patient's categories. Our study investigated the facial nerve at a single anatomical point. We may hypothesize that a multiple-point assessment might increase the reliability of facial nerve HRUS. Further studies, including larger samples of patients assessing the nerve diameter at multiple points, are needed to provide reliable

reference values and support conclusive information on the predictive value of facial nerve HRUS in patients with Bell's palsy. Moreover, the combination of nerve ultrasound and neurophysiological data in larger samples of patients with Bell's palsy may potentially improve prognostication in patients with Bell's Palsy. In our participants, the difference in the facial nerve diameter median values between the affected and healthy sides is relatively small. This observation is in line with previous studies (Baek et al., 2020; Tawfik et al., 2015a) and reflects the large variability of facial nerve diameter in the affected side of patients with Bell's palsy (some patients had a mild/negligible increase of the diameter). In our study, we have therefore used the facial nerve diameter asymmetry parameter ((diameter affected-diameter control side)/diameter control side*100), which is probably more reliable for the assessment at a single subject level. The first neurophysiological and nerve ultrasound evaluations were performed after 10–15 days after the diagnosis, after the corticosteroid treatment. We cannot exclude that treatment may impact our findings (e.g., a persistent post-treatment nerve enlargement may reflect more severe facial nerve damage).

5.Conclusions

Our longitudinal study shows that facial nerve HRUS demonstrates an increased facial nerve diameter in the acute phase of Bell's palsy, thus potentially improving patients' evaluation. The negative predictive value of facial nerve HRUS examination in the acute phase of facial nerve palsy is relatively high, thus potentially supporting the usefulness of this technique in the diagnostic pathway of Bell's palsy. However, facial nerve HRUS examination has a poorer prognostic value than facial nerve conduction study in patients with Bell's palsy.

Table 1. House-Brackmann Score, Neurophysiological and Ultrasound variables across three time points.

	Side	**T1 (n=34)**	**T2 (n=31)**	**T3 (n=31)**
House-Brackmann score	Affected	4 (3-4)	2 (2-3)	1 (1-2)
Neurophysiological variables				
CMAP latency (ms)	Affected	3.6 (3.1-4.4)	3.6 (3.2-4)	3.3 (3-3.8)
	Control	3 (2.6-3.3)	3.2 (2.8-3.6)	3.1 (2.8-3.6)

CMAP Amplitude (mV)	Affected	1.2 (0.8-1.75)	1.7 (0.9-2)	2 (1.5-2.5)
	Control	2.5 (2-3)	2.5 (2-3)	2.6 (2-3)
R1 blink reflex preserved	Affected	23	27	27
EMG denervation	Affected	1	4	0
High Resolution Nerve Ultrasound				
Facial nerve diameter (mm)	Affected	0.8 (0.7-1.1)	0.8 (0.6-1)	0.7 (0.6-1)
	Control	0.7 (0.6-1)	0.7 (0.5-0.9)	0.7 (0.6-1)

CMAP: compound muscle action potential

CMAP and ultrasound variables are expressed as median and (IQR); R1 blink reflex and EMG denervation are expressed as absolute number of patients

Table 2. Comparison between patients with complete (HB=1) and incomplete (HB>1) recovery at one months (T2).

	Complete recovery HB=1 (n=7)	**Incomplete recovery HB>1 (n=24)**	**p**
Age (years)	45 (23; 70)	55.5 (42.25; 63)	0.72
Sex (M:F)	1:6	12:12	0.19
HB at T1	4 (3; 4)	4 (3; 4)	0.27
Preserved R1 blink reflex at T1	7	14	0.06
CMAP on the affected side at T1 (mV)	1.6 (1.2; 2.2)	1.15 (0.62; 1.85)	0.17
Facial nerve diameter on the affected side at T1 (mm)	0.6 (0.5; 0.8)	0.9 (0.7; 1.22)	0.023
CMAP amplitude asymmetry at T1 (%)	-40 (-45; -27.27)	-55 (-77.62; -25.95)	0.19

Facial nerve diameter asymmetry at T1 (%)	0 (-19.64; 9.37)	24 (0; 34.3)	0.035

HB: House-Brackmann score

Values are expressed as: Median (IQR)

p assessed by Mann-Whitney test and chi-squared test and Fisher's exact test as appropriate

Preserved R1 blink reflex is expressed as absolute number of patients

CMAP: compound muscle action potential

CMAP amplitude asymmetry: (CMAP amplitude affected - CMAP amplitude control side)/CMAP amplitude control side*100

Facial nerve diameter asymmetry: (diameter affected-diameter control side)/diameter control side*100

Table 3. Comparison between patients with complete (HB=1) and incomplete (HB>1) recovery at three months (T3).

	Complete recovery HB=1 (n=20)	**Incomplete recovery HB>1 (n=11)**	**p**
Age (years)	45 (23; 70)	60 (55; 68)	0.02
Sex (M:F)	7:13	6:5	0.44
HB at T1	4 (3; 4)	4 (4; 6)	0.03
Preserved R1 blink reflex at T1	16	5	0.1
CMAP on the affected side at T1 (mV)	1.6 (1.2; 2.15)	0.6 (0.5; 1)	<0.001
Facial nerve diameter on the affected side at T1 (mm)	0.75 (0.62; 1)	0.9 (0.7; 1.3)	0.16
CMAP amplitude asymmetry at T1 (%)	-35.8 (-49.4; -23.43)	-77.78 (-84;-62.9)	<0.001
Facial nerve diameter asymmetry at T1 (%)	0 (0; 27.5)	30 (14.29; 50)	0.014

HB: House-Brackmann score

Values are expressed as: Median (IQR)

p assessed by Mann-Whitney test and chi-squared test and Fisher's exact test as appropriate

Preserved R1 blink reflex is expressed as as absolute number of patients

CMAP: compound muscle action potential

CMAP amplitude asymmetry: CMAP amplitude affected - CMAP amplitude control side/CMAP amplitude control side*100

Facial nerve diameter asymmetry: diameter affected-diameter control side)/diameter control side*100

Table 4. Comparison between patients with complete (HB=1) and incomplete (HB>1) recovery at six months (T4).

	Complete recovery HB=1 (n=24)	**Incomplete recovery HB>1 (n=7)**	**p**
Age (years)	48 (35.7; 63)	55 (60; 73)	0.03
Sex (M:F)	8:16	5:2	0.1
HB at T1	4 (3;4)	4 (4; 6)	0.008
Preserved R1 blink reflex at T1	19	2	0.02
CMAP on the affected side at T1 (mV)	1.45 (1.12; 1.97)	0.6 (0.4; 0.9)	<0.001
Facial nerve diameter on the affected side at T1 (mm)	0.8 (0.7; 1)	0.9 (0.7; 1.3)	0.23
CMAP amplitude asymmetry at T1 (%)	-38.33 (-57.5; -24.4)	-77.78 (-84; -71.88)	<0.001

Facial nerve diameter asymmetry at T1 (%)	0 (0; 27.5)	30 (28.57; 50)	0.016

HB: House-Brackmann score

Values are expressed as: Median (IQR)

p assessed by Mann-Whitney test and chi-squared test and Fisher's exact test as appropriate

Preserved R1 blink reflex is expressed as absolute number of patients

CMAP: compound muscle action potential

CMAP amplitude asymmetry: CMAP amplitude affected - CMAP amplitude control side/CMAP amplitude control side*100

Facial nerve diameter asymmetry: diameter affected-diameter control side)/diameter control side*100

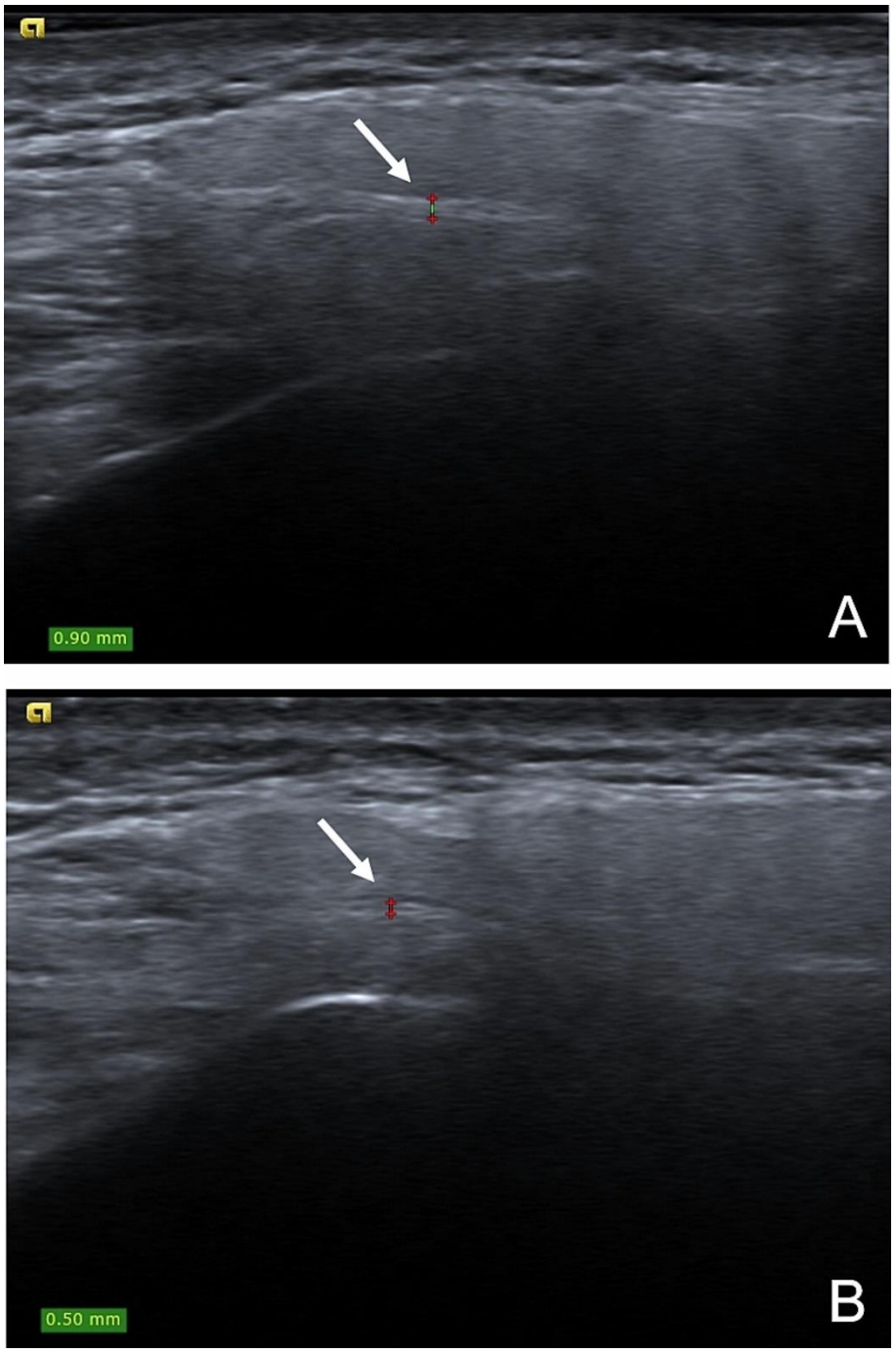

Figure 1. Facial Nerve Ultrasound at T1 in a representative patient: A. Affected side, B. Control side.

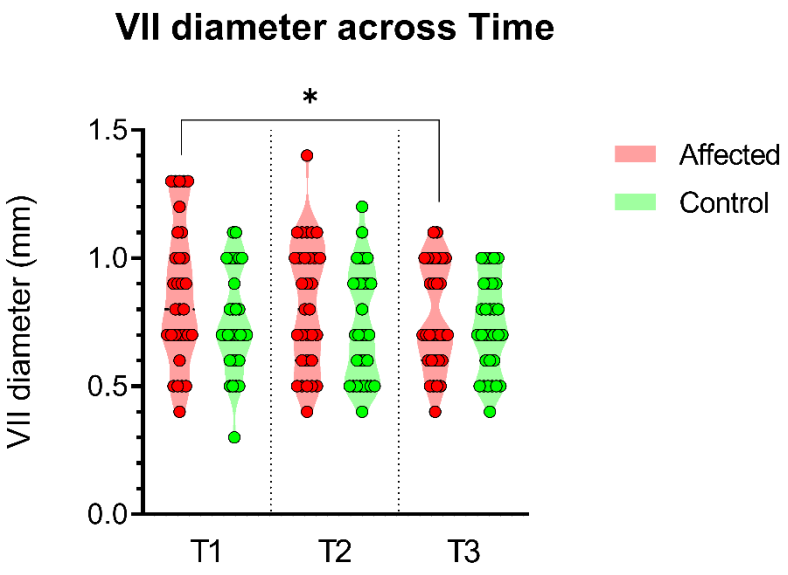

Figure 2. Two-way repeated measure ANOVA, for the facial nerve diameter. The asterisks indicate a significant difference (post hoc analysis with Sidak correction) between facial nerve diameter at T1 and T3 (p=0.005).

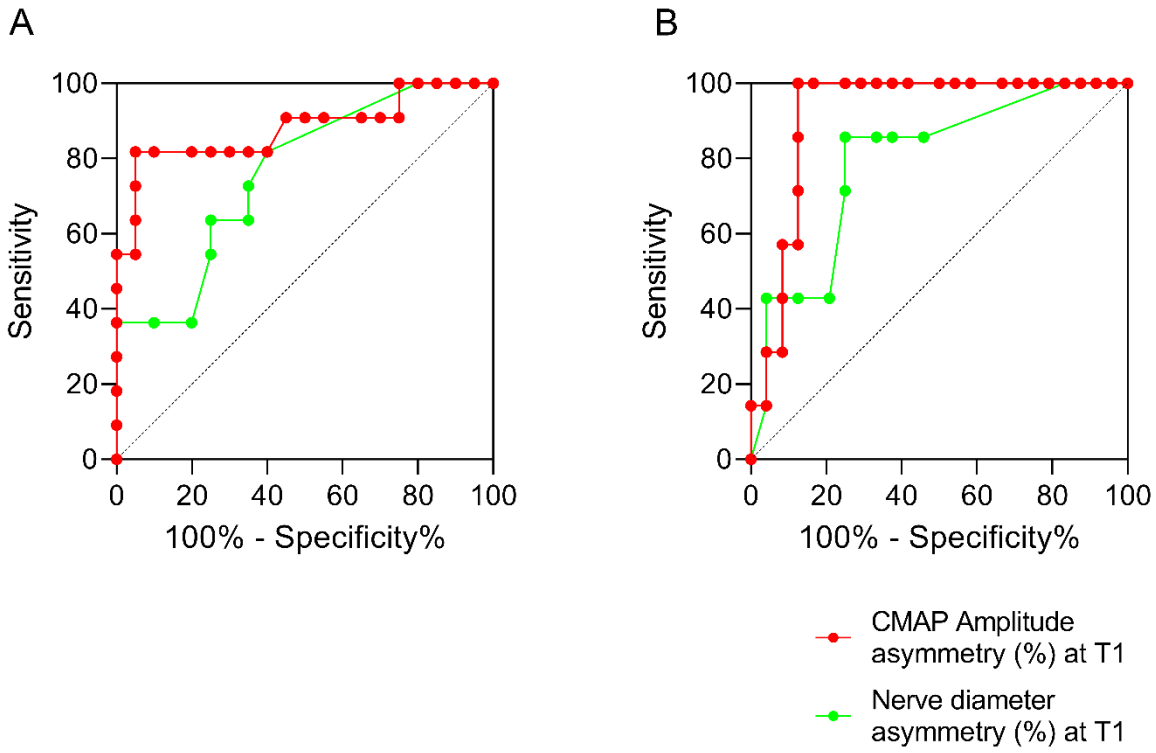

Figure 3. ROC curve analysis after three (A) and six (B) months from symptoms onset. Red dots: side-to-side facial nerve compound muscle action potential (CMAP) amplitude asymmetry using the contralateral side as reference. Green dots: side-to-side facial nerve diameter asymmetry using the contralateral side as reference.

Optimal trade-off value between sensitivity and specificity corresponded to a facial nerve diameter asymmetry of 25% (an increase in the diameter on the affected side higher than the 25% of the control side) and a CMAP amplitude asymmetry of 65% (a decrease in the CMAP amplitude on the affected side more than the 65% of the control side).

Supplementary table 1. Clinical data of patients with Bell's Palsy at T1.

	Patients, n=34
Age (years)	55 (40-65)
Sex M:F	16:18
House-Brackmann score at T1	4 (3-4)
Time from disease onset to steroids treatment (hours)	24 (23-42)
Non motor symptoms	
Auricular pain	25 (73.5%)
Dry eye	17 (50%)
Hyperacusis	11 (32.3%)
Dysgeusia	13 (38.2%)
Comorbidities	
Hypertension	7 (20.5%)
Thyreopathy	3 (8.8%)

Age, House-Brackmann score and time from disease onset to steroids treatment are expressed as median and (IQR); non-motor symptoms and comorbidities are expressed as absolute number of patients' value and (frequency in %).

References

Baek, S.-H., Kim, Y.H., Kwon, Y.-J., Sung, J.H., Son, M.H., Lee, J.H., Kim, B.-J., 2020. The Utility of Facial Nerve Ultrasonography in Bell's Palsy. Otolaryngol. Neck Surg. 162, 186–192. https://doi.org/10.1177/0194599819896298

De Seta, D., Mancini, P., Minni, A., Prosperini, L., De Seta, E., Attanasio, G., Covelli, E., De Carlo, A., Filipo, R., 2014. Bell's Palsy: Symptoms Preceding and Accompanying the Facial Paresis. Sci. World J. 2014, 1–6. https://doi.org/10.1155/2014/801971

Eviston, T.J., Croxson, G.R., Kennedy, P.G.E., Hadlock, T., Krishnan, A.V., 2015. Bell's palsy: aetiology, clinical features and multidisciplinary care. J. Neurol. Neurosurg. Psychiatry 86, 1356–1361. https://doi.org/10.1136/jnnp-2014-309563

Halvorson, D.J., Coker, N.J., Wang-Bennett, L.T., 1993. Histologic correlation of the degenerating facial nerve with electroneurography. The Laryngoscope 103, 178–184. https://doi.org/10.1002/lary.5541030210

House JW, Brackmann DE. Facial nerve grading system. Otolaryngol Head Neck Surg. 1985 Apr;93(2):146-7. doi: 10.1177/019459988509300202.

Hsueh, H.-W., Chang, K.-C., Chao, C.-C., Hsieh, S.-T., 2020. A Pilot Study on Serial Nerve Ultrasound in Miller Fisher Syndrome. Front. Neurol. 11, 865. https://doi.org/10.3389/fneur.2020.00865

Kerasnoudis, A., Pitarokoili, K., Behrendt, V., Gold, R., Yoon, M.-S., 2015. Correlation of Nerve Ultrasound, Electrophysiological and Clinical Findings in Chronic Inflammatory Demyelinating Polyneuropathy: Nerve Ultrasound Findings in Chronic Inflammatory Demyelinating Polyneuropathy. J. Neuroimaging 25, 207–216. https://doi.org/10.1111/jon.12079

Kimura, J., Giron, L.T., Young, S.M., 1976. Electrophysiological Study of Bell Palsy: Electrically Elicited Blink Reflex in Assessment of Prognosis. Arch. Otolaryngol. - Head Neck Surg. 102, 140–143. https://doi.org/10.1001/archotol.1976.00780080062005

Li, S., Guo, R.-J., Liang, X.-N., Wu, Y., Cao, W., Zhang, Z.-P., Zhao, W., Liang, H.-D., 2016. High-frequency ultrasound as an adjunct to neural electrophysiology: Evaluation and prognosis of Bell's palsy. Exp. Ther. Med. 11, 77–82. https://doi.org/10.3892/etm.2015.2878

Liston, S.L., Kleid, M.S., 1989. Histopathology of Bell's palsy. The Laryngoscope 99, 23–26. https://doi.org/10.1288/00005537-198901000-00006

Lo, Y.L., Fook-Chong, S., Leoh, T.H., Dan, Y.F., Lee, M.P., Gan, H.Y., Chan, L.L., 2010. High-resolution ultrasound in the evaluation and prognosis of Bell's palsy: Ultrasound and Bell's palsy. Eur. J. Neurol. 17, 885–889. https://doi.org/10.1111/j.1468-1331.2010.02950.x

Michaels, L., 1990. Histopathological Changes in the Temporal Bone in Bell's Palsy. Acta Otolaryngol. (Stockh.) 109, 114–118. https://doi.org/10.3109/00016488909138364

Ozgur, A., Semai, B., Hidir, U.U., Mehmet Fatih, O., Tayfun, K., Zeki, O., 2010. Which electrophysiological measure is appropriate in predicting prognosis of facial paralysis? Clin. Neurol. Neurosurg. 112, 844–848. https://doi.org/10.1016/j.clineuro.2010.07.001

Tawfik, E.A., Walker, F.O., Cartwright, M.S., 2015a. Neuromuscular Ultrasound of Cranial Nerves. J. Clin. Neurol. 11, 109. https://doi.org/10.3988/jcn.2015.11.2.109

Tawfik, E.A., Walker, F.O., Cartwright, M.S., 2015b. A Pilot Study of Diagnostic Neuromuscular Ultrasound in Bell's Palsy: Facial Nerve Ultrasound. J. Neuroimaging 25, 564–570. https://doi.org/10.1111/jon.12269

Valls-Solé, J., 2007. Electrodiagnostic studies of the facial nerve in peripheral facial palsy and hemifacial spasm. Muscle Nerve 36, 14–20. https://doi.org/10.1002/mus.20770

Van den Bergh, P.Y.K., Doorn, P.A., Hadden, R.D.M., Avau, B., Vankrunkelsven, P., Allen, J.A., Attarian, S., Blomkwist-Markens, P.H., Cornblath, D.R., Eftimov, F., Goedee, H.S., Harbo, T., Kuwabara, S., Lewis, R.A., Lunn, M.P., Nobile-Orazio, E., Querol, L., Rajabally, Y.A., Sommer, C., Topaloglu, H.A., 2021. European Academy of Neurology/Peripheral Nerve Society guideline on diagnosis and treatment of chronic inflammatory demyelinating polyradiculoneuropathy: Report of a joint Task Force—Second revision. Eur. J. Neurol. 28, 3556–3583. https://doi.org/10.1111/ene.14959

Walker, F.O., Cartwright, M.S., Alter, K.E., Visser, L.H., Hobson-Webb, L.D., Padua, L., Strakowski, J.A., Preston, D.C., Boon, A.J., Axer, H., van Alfen, N., Tawfik, E.A., Wilder-Smith, E., Yoon, J.S., Kim, B.-J., Breiner, A., Bland, J.D.P., Grimm, A., Zaidman, C.M., 2018. Indications for neuromuscular ultrasound: Expert opinion and review of the literature. Clin. Neurophysiol. 129, 2658–2679. https://doi.org/10.1016/j.clinph.2018.09.013

Yoo, M.C., Soh, Y., Chon, J., Lee, J.H., Jung, J., Kim, S.S., You, M.-W., Byun, J.Y., Kim, S.H., Yeo, S.G., 2020. Evaluation of Factors Associated With Favorable Outcomes in Adults With Bell Palsy. JAMA Otolaryngol. Neck Surg. 146, 256. https://doi.org/10.1001/jamaoto.2019.4312

Study 2 - Nerve Ultrasound in Friedreich's Ataxia: enlarged nerves as a biomarker of disease severity

Clin Neurophysiol. 2024 Feb 2:159:75-80. doi: 10.1016/j.clinph.2024.01.004.

Abstract

Objective: In Friedreich's ataxia research, the focus is on discovering treatments and biomarkers to assess disease severity and treatment effects. Our study examines high-resolution nerve ultrasound in these patients, seeking correlations with established clinical markers of disease severity.

Method: Ten patients with Friedreich's Ataxia underwent a comprehensive clinical assessment with established scales (SARA, FARS, mFARS, INCAT, ADL 0-36, IADL). Additionally, they underwent nerve conduction studies and high-resolution nerve ultrasound. Quantitative evaluation of nerve cross-sectional area, conducted at 24 nerve sites using high-resolution nerve ultrasound, was compared with data obtained from 20 healthy volunteers.

Results: All the patients had a severe sensory axonal neuropathy. High-resolution nerve ultrasound showed significant increase, in cross sectional area, of median and ulnar nerves at the axilla and arm. The cumulative count of affected nerve sites was directly associated with clinical disability, as determined by SARA, FARS, mFARS, ADL 0-36, and INCAT score, while displaying an inverse correlation with IADL.

Conclusions: Our study shows that high-resolution ultrasound reveals notable nerve abnormalities, primarily in the upper limbs of patients diagnosed with Friedreich's Ataxia. The observed correlation between these nerve abnormalities and clinical disability scales indicates the potential use of this technique as a biomarker for evaluating disease severity and treatment effects.

Significance: Nerve Ultrasound is a potential biomarker of disease severity in Friedreich's Ataxia.

Keywords: Biomarker; Friedreich's Ataxia; Nerve Ultrasound.

1 Introduction

Friedreich's ataxia caused by GAA expansions within the FXN gene, stands as the most prevalent form of hereditary ataxia, inherited in an autosomal recessive manner. *FXN* encodes for Frataxin, a pivotal mitochondrial protein involved in iron methabolism. Longer trinucleotide expansions have been linked to more severe phenotypes, with early onset (<25 years), and a higher risk of mortality (Bürk, 2017; Rummey et al., 2022).

Friedreich's ataxia is a multisystem disorder, affecting Central and Peripheral Nervous Systems as well as the heart, skeleton, and endocrine pancreas. Mutations in *FXN* gene particularly result in damage to the Peripheral Nervous System, leading to sensory neuropathy, a primary hallmark of Friedreich's ataxia (Koeppen, 2011).

Clinical research is actively pursuing potential treatments to advance patient care significantly. Therefore, there is a growing emphasis on identifying potential biomarkers to effectively evaluate disease severity and treatment effects. While nerve conduction studies can effectively identify sensory neuropathy in Friedreich's ataxia, sensory nerve action potentials are often significantly reduced or completely absent. This occurrence suggests a floor effect, thus limiting the ability of nerve conduction study to measure disease severity or treatment effects, thus diminishing its potential as a biomarker in patients with Friedreich's ataxia (Creigh et al., 2019).

Having a readily available and reliable biomarker capable of highlighting and measuring disease severity or treatment effects would significantly enhance our ability to identify effective therapeutic strategies for this rare condition (Gavriilaki et al., 2023). In the process of identifying a reliable biomarker in Friedreich's ataxia, a critical step involves validating how the potential biomarker correlates with clinically established variables.

High-resolution nerve ultrasound is increasingly used as tool for investigating conditions affecting the peripheral nervous system. This technique provides useful structural and anatomic information in different peripheral nervous system diseases (Walker, 2017). However, its usefulness in assessing peripheral neuropathy associated with Friedreich's ataxia remains a largely unexplored research area. Accordingly, the reliability of High-resolution ultrasound examination in reflecting clinical variables and its potential use as a biomarker in Friedreich's ataxia remain unclear.

In this study, our aim was to investigate whether high-resolution nerve ultrasound might serve as a potential biomarker in patients with Friedreich's ataxia. To do so, we examined the nerve cross-sectional area (CSA) using high-resolution nerve ultrasound in patients with Friedreich's ataxia and investigated its correlation with disease severity as assessed with clinically established variables.

2 Methods

2.1 Study cohort and design

Between January 1, 2022, and December 31, 2022, we conducted a prospective enrolment of a consecutive series of patients at the Rare Neurological Diseases Unit (Department of Medico-Surgical Sciences and Biotechnologies, University Sapienza, Latina) who were genetically confirmed to have Friedreich's Ataxia. The study took place at the Peripheral Neuropathy and Neuropathic Pain Unit within the Department of Human Neuroscience at Sapienza University, Rome. On the same day, all patients underwent a comprehensive neurological examination, Nerve Conduction Study, and High-Resolution Ultrasound examination.

Data collection was meticulously carried out using structured forms and standardized protocols, with the involvement of dedicated staff members. The clinical examination was performed by AT, CC, and EC, the nerve conduction study by EG and GDS, and the high-resolution nerve ultrasound examination by GDP and PF.

Prior to their participation, all patients provided written informed consent. The research adhered to the principles outlined in the Declaration of Helsinki and its later amendments, and it received approval from the institutional ethics committee.

2.2 Clinical evaluation

Demographic and clinical data, including age, gender, comorbidities, and disease duration, were systematically collected. Each patient also underwent a comprehensive neurological examination, which included the assessment of clinical and functional scales, including the Scale for the Assessment and Rating of Ataxia (SARA), Friedreich’s Ataxia Rating Scale (FARS), modified FARS (mFARS), the Inflammatory Neuropathy Cause and Treatment Disability Score (INCAT), the Activities of Daily Living (ADL 0-36 score) and the Instrumental Activities of Daily Living (IADL).

SARA is an 8-items scale providing a total score ranging from 0 (no ataxia) to 40 (severe ataxia) (Yabe et al., 2008). FARS and mFARS are neurological scales where higher scores correspond to higher severity; the total score (maximum score: 125 for FARS and 93 for mFARS) is obtained by the sum of five subscales (bulbar function, upper limb coordination, lower limb coordination, peripheral nervous system, and upright stability) (Rummey et al., 2022). INCAT was assessed at the upper limb ranging from 0 (not affected) to 5 (prevented to perform specific tasks) and at the lower limb ranging from 0 (walks without difficulty) to 5 (confined to wheelchair). The overall INCAT disability score sums the upper and lower limb scores (Merkies et al., 2000). Quantification of daily life activities was estimated by the ADL, score ranging from 0 (normal function) to 36 (severe functional disability) (Lynch et al., 2006). IADL is an 8-items questionnaires that measure the degree of independence and the ability to perform the skills of daily living, the final score ranges from 8 (high function) to 0 (low function) (Edemekong et al., 2022).

2.3 Nerve Conduction Study

Nerve conduction study was performed using surface recording electrodes following the recommendations of the International Federation of Clinical Neurophysiology (Kimura J, 2006). We studied sensory nerve action potentials and conduction velocities of sural, median, ulnar, and superficial radial nerves; compound muscle action potentials and conduction velocities of peroneal, tibial, median and ulnar nerves. Skin temperature was kept between 32°C and 34°C. Nerve conduction study data were compared with the age-matched normative ranges established in our laboratory.

2.4 High-Resolution Nerve Ultrasound

High-resolution nerve ultrasound examination (MyLabX8, Esaote, Genova, Italy) was performed with a broadband linear transducer (frequency band 5-15 MHz). Median, ulnar, peroneal, tibial and sural nerves were followed along their anatomical course bilaterally. For each patient we evaluated a total of 24 nerve sites. The CSA of each nerve segment was measured at the most enlarged nerve point using the ellipse technique or the area tracing, when the nerve had an irregular shape, at: axilla, arm, forearm, wrist, popliteal fossa, fibular head and calf. High-resolution nerve ultrasound findings in patients with Friedreich's ataxia were compared with a control group of 20 healthy subjects.

For each patient we calculated a total number of altered nerve sites as the numerical sum of the detected abnormal sites considering axilla, arm, forearm, popliteal fossa, and calf bilaterally. Nerve

segments with a nerve CSA within our laboratory range values were considered normal. In the assessment of the total number of altered nerve sites we excluded common entrapment sites, to avoid a possible bias due to entrapment neuropathies.

2.5 Statistical analysis

Since most variables had a non-normal distribution as assessed by Kolmogorov-Smirnov test we used nonparametric tests. Fisher's exact test was used to test the association between categorical variables. For the statistical analysis we considered each nerve on its own; CSA values between Friedreich's ataxia and controls were compared with the Kruskal-Wallis test with Dunn's multiple comparison test for nerves with multiple scanning sites (median, ulnar, peroneal nerves) and Mann-Whitney test for nerves with a single scanning point (tibial and sural nerves). The association between clinical and high-resolution nerve ultrasound findings was assessed by Spearman correlation. Statistical analyses were performed with GraphPad Prism 9.5 (GraphPad Software, Inc., San Diego, CA).

3 Results

Ten patients with Friedreich's ataxia (Table 1) and twenty healthy controls were enrolled. None of these participants had possible causes of acquired peripheral neuropathy. All the patients had a sensory axonal neuropathy, while one patient had severe reduction of all sensory action potentials, the other nine patients had absent sensory nerve action potentials. Motor nerve compound muscle action potentials and motor conduction velocities were within normal ranges in all patients.

In the comparison between patients with Friedreich's ataxia and healthy participants, high-resolution nerve ultrasound examination showed statistically significant enlargement of the median ($p<0.001$, using the Kruskal-Wallis Test with Dunn's multiple comparisons test) and ulnar ($p<0.001$, using the Kruskal-Wallis Test with Dunn's multiple comparisons test) nerves, both at the axilla and arm locations (Table 2, Figure 1, Figure 2, Figure 3). High-resolution nerve ultrasound findings are summarized in Table 2.

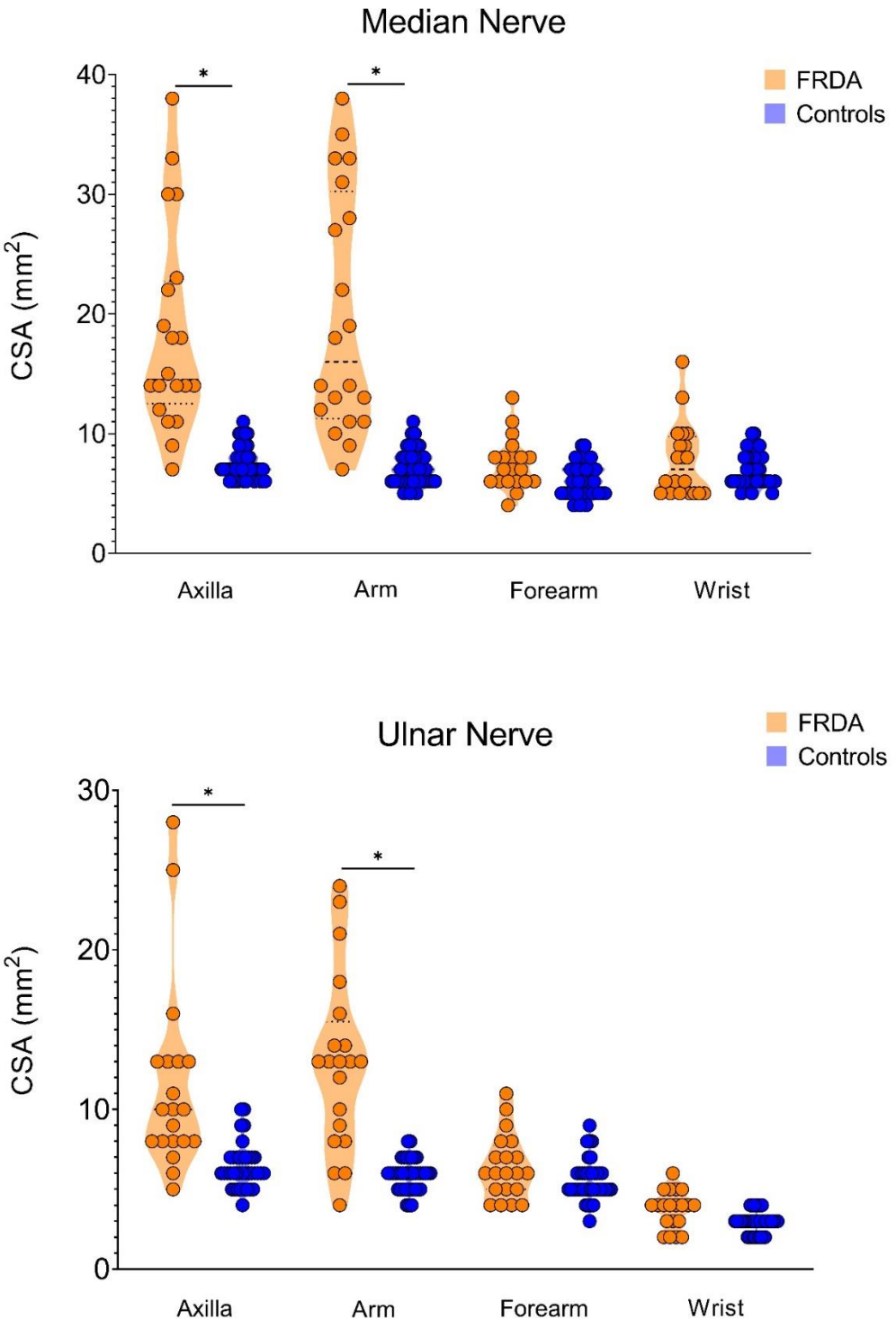

Figure 1. Cross Sectional Area of Median and Ulnar nerves as assessed with high resolution nerve ultrasound examination in patients with Friedreich's ataxia (orange) and control participants (blue).

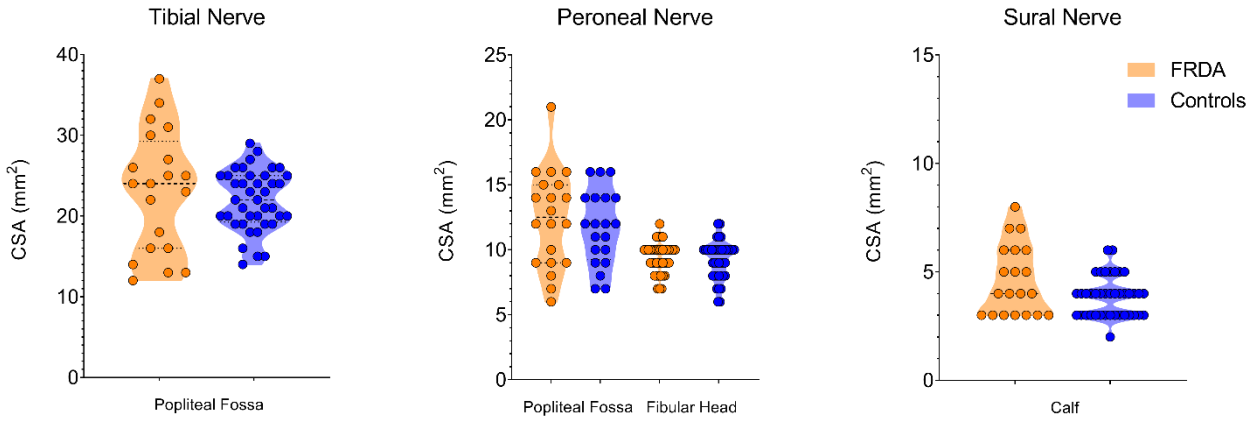

Figure 2. Cross Sectional Area of Tibial, Peroneal and Sural nerves as assessed with high resolution nerve ultrasound examination in patients with Friedreich's ataxia (orange) and control participants (blue).

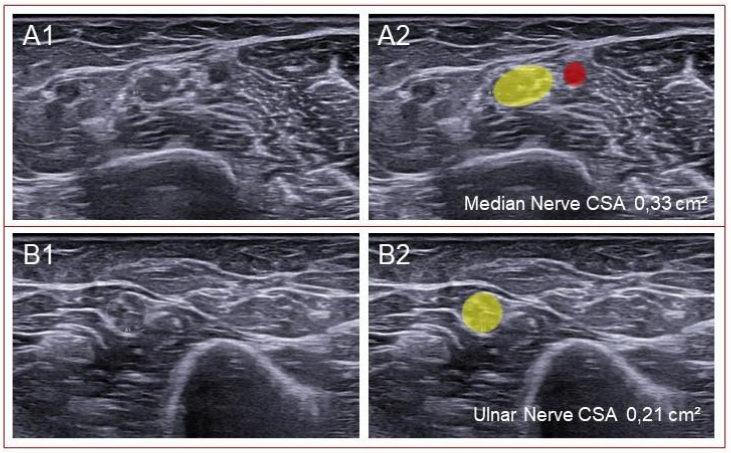

Figure 3. High resolution nerve ultrasound examination showing an enlarged Median (A) and Ulnar (B) nerves at the arm in Friedreich's ataxia. Yellow circles indicate the nerves and red circles indicate the artery.

The total number of abnormal nerve sites positively correlated with SARA, FARS, mFARS, INCAT and ADL scores, and inversely correlated with IADL (the more severe the clinical and functional symptoms, the more extensive the nerve damage) (Table 3). Conversely, GAA repeats in the shorter of the two alleles and the disease duration did not correlate with the total number of altered nerve sites ($p=0.75$ and $p=0.072$, respectively).

4 Discussion

In the present study, we showed that high-resolution ultrasound examination detected specific nerve abnormalities in patients with Friedreich's ataxia. These abnormalities correlated with clinically established variables thus indicating the potential of high-resolution nerve ultrasound as a sensitive biomarker in Friedreich's ataxia.

In our patients with Friedreich's ataxia, high-resolution nerve ultrasound examination showed an increased CSA in multiple nerves. This finding appears to contradict the common assumption that sensory neuropathy, in Friedreich's ataxia, is primarily a ganglionopathy. Considering that sensory axons constitute more than 90% of the total axons in a mixed nerve (Gesslbauer et al., 2017), a pure sensory neuronopathy would typically result in a reduction in nerve size (Leadbetter et al., 2019; van Alfen, 2019). However, frataxin is expressed in Schwann cells and its deficiency leads to cell death by activating inflammatory pathways, thus leading to peripheral nerve oedema and inflammation potentially resulting in the observed nerve enlargement (Lu et al., 2009; McLeod, 1971).

The detection of nerve enlargement, in combination with severe sensory axonal loss at nerve conduction study, is a peculiar finding. Conventionally, nerve enlargement is a characteristic feature in acquired and genetic demyelinating neuropathies (Grimm et al., 2017; Lucchetta et al., 2011), while axonal neuropathies typically show minimal or no nerve swelling (Grimm et al., 2014). Limited research has highlighted increased nerve CSA in specific axonal neuropathies (Leonardi et al., 2022; Salvalaggio et al., 2020). This emphasizes the significance of our findings in the context of Friedreich's ataxia.

We found an increased nerve CSA, especially at the upper limbs. This finding may reflect a differential involvement of upper and lower limb sensory neurons in patients with Friedreich's ataxia, as observed at the spinal cord level, where the gracile fasciculus is more severely affected (Koeppen, 2011). Accordingly, the lack of detectable high-resolution nerve ultrasound alterations at the lower limbs may be the consequence of a long-standing nerve damage where atrophy and regeneration phenomena coexist (Caruso et al., 1983; Koeppen, 2011).

In our cohort, an observed increase in CSA using nerve ultrasound aligns with both clinical severity and functional disability. Notably, high-resolution nerve ultrasound examination proves to be valuable in situations where nerve conduction studies might lack meaningful insights. As novel disease-modifying drugs for Friedreich's ataxia are under exploration (Lynch et al., 2006; Zesiewicz et al., 2020), high-resolution nerve ultrasound examination emerges as a promising and reliable biomarker for assessing treatment effects. Future longitudinal studies in patients with Friedreich's ataxia could explore the potential of nerve CSA as assessed with high-resolution ultrasound as a valid surrogate endpoint, objectively reflecting changes in patient outcomes or condition.

Our study strengthens the significance of high-resolution nerve ultrasound as a complementary tool to nerve conduction studies, offering support in investigating peripheral nervous system diseases. Building upon and expanding previous research using high-resolution nerve ultrasound in small Friedreich's ataxia patient groups, our study presents a comprehensive analysis of clinical, neurophysiological, and ultrasound findings within a larger patient cohort. Notably, we employed a more detailed ultrasound protocol compared to earlier studies (Mulroy et al., 2018; Salvalaggio et al., 2015).

Limitations

We examined the correlation between nerve CSA and clinical variables in a cohort of ten patients. It follows that our findings might have a limited generalizability due to the small sample size. Nevertheless, among these ten patients, we observed a consistent correlation between nerve CSA and all the different clinical variables we assessed.

Given that high-resolution nerve ultrasound examination is operator-dependent, the reproducibility of this technique remains an open issue, potentially impacting our findings. Nonetheless, our study

implemented a standardized ultrasound protocol, leading to improved reproducibility (Di Pietro et al., 2023).

In our study, we focused primarily on a nerve parameter—namely, the nerve CSA—due to its high reproducibility and reliability in nerve high-resolution ultrasound measures (Fisse et al., 2021). However, it is worth noting that the inclusion of additional parameters, such as nerve echogenicity and vascularity, cannot be ruled out and might enhance the diagnostic utility of high-resolution nerve ultrasound.

5 Conclusions

Our study now shows that high-resolution nerve ultrasound examination can detect nerve enlargements in patients with Friedreich's ataxia (mostly at the level of upper limbs).

Neve ultrasound abnormalities correlate with clinically established variables in patients with Friedreich's ataxia. This technique, therefore, might be a promising biomarker for measuring disease severity and treatment effects in this rare and severely disabling condition.

Table 1. Clinical data in patients with Friedreich's ataxia.

	Patients, n=10
Age (years)	40 (29-44.8)
Sex (M:F)	2:8
Disease Duration (years)	21 (8.8-27.8)
Trinucleotide Repeat Length (GAA1)	598 (415-795)
Clinical Scales	
SARA	28.5 (10.8-30.5)
FARS	68.75 (48.1-73.4)
mFARS	62.25 (43.9-65.1)

INCAT Arm	3 (2-4)	
INCAT Leg	4 (1-5)	
INCAT Total	8 (3-8.2)	Values are expressed as median (IQR) GAA1: the shorter of the two alleles SARA: Scale for the Assessment and
ADL	28.5 (11.3-30)	
IADL	3 (2-8)	

Rating of Ataxia
FARS: Friedreich's Ataxia Rating Scale
mFARS: modified Friedreich's Ataxia Rating Scale
INCAT: Inflammatory Neuropathy Cause and Treatment Disability Score
ADL: Activities of Daily Living 0-36 score
IADL: Instrumental Activities of Daily Living

Table 2. Nerve cross sectional area (mm^2) as assessed with high resolution ultrasound.

	Patients, n=10	**Controls, n=20**	**p***
Median Nerve			
Axilla	14.5 (12.5-22.75)	7 (7-9)	**0.0007**
Arm	16 (11.25-30.25)	7 (6-8)	**<0.0001**
Forearm	7 (6-8)	6 (5-7)	0.32
Wrist	7 (5-9.75)	7 (6-8)	0.1
Ulnar Nerve			
Axilla	10 (8-13)	7 (7-9)	**0.0002**
Arm	13 (8.25-15.5)	7 (6-8)	**<0.0001**
Forearm	6 (5-7.75)	5 (5-6)	0.604
Wrist	4 (3-4.75)	3 (2.25-3)	0.1

Peroneal Nerve			
Popliteal fossa	12.5 (9-15)	10 (8-10)	0.109
Caput fibulae	12 (9.25-14)	10 (9-10)	0.202
Tibial Nerve			
Popliteal fossa	24 (16-29.25)	22 (19.25-25)	0.545
Sural Nerve			
Calf	4 (3-6)	4 (3-4)	0.125

Values are expressed as median (IQR)
CSA Cross Sectional Area
*by Kruskal-Wallis test with Dunn's multiple comparison test for Median, Ulnar and Peroneal nerves; by Mann-Whitney test for Tibial and Sural nerves

Table 3. Correlations between the Total Number of Altered nerve Sites and clinical scales.

	Spearman r	**p**
TNAS vs SARA	0.709	0.026
TNAS vs FARS	0.740	0.018
TNAS vs mFARS	0.758	0.014
TNAS vs INCAT	0.648	0.048
TNAS vs ADL	0.674	0.038
TNAS vs IADL	-0.758	0.015

TNAS: Total Number of Altered nerve Sites (median nerve at axilla, arm and forearm; ulnar nerve at axilla, arm and forearm; peroneal and tibial nerves at popliteal fossa and sural nerve at calf bilaterally).
SARA: Scale for the Assessment and Rating of Ataxia.
FARS: Friedreich's Ataxia Rating Scale.
mFARS: modified Friedreich's Ataxia Rating Scale.
INCAT: Inflammatory Neuropathy Cause and Treatment Disability Score.
ADL: Activities of Daily Living 0-36 score.
IADL: Instrumental Activities of Daily Living.

References

Bürk, K., 2017. Friedreich Ataxia: current status and future prospects. Cerebellum Ataxias 4, 4. https://doi.org/10.1186/s40673-017-0062-x

Caruso, G., Santoro, L., Perretti, A., Serlenga, L., Crisci, C., Ragno, M., Barbieri, F., Filla, A., 1983. Friedreich's ataxia: electrophysiological and histological findings. Acta Neurol. Scand. 67, 26–40. https://doi.org/10.1111/j.1600-0404.1983.tb04542.x

Creigh, P.D., Mountain, J., Sowden, J.E., Eichinger, K., Ravina, B., Larkindale, J., Herrmann, D.N., 2019. Measuring peripheral nerve involvement in Friedreich's ataxia. Ann. Clin. Transl. Neurol. 6, 1718–1727. https://doi.org/10.1002/acn3.50865

Di Pietro, G., Falco, P., D'Elia, C., Cavalcanti, L., De Stefano, G., Di Stefano, G., Fabiano, E., Galosi, E., Leone, C., Vicenzini, E., Truini, A., Mancini, P., 2023. Predicting value for incomplete recovery in Bell's palsy of facial nerve ultrasound versus nerve conduction study. Clin. Neurophysiol. S1388245723007964. https://doi.org/10.1016/j.clinph.2023.11.020

Edemekong, P.F., Bomgaars, D.L., Sukumaran, S., Schoo, C., 2022. Activities of Daily Living, in: StatPearls. StatPearls Publishing, Treasure Island (FL).

Fisse, A.L., Katsanos, A.H., Gold, R., Pitarokoili, K., Krogias, C., 2021. Cross-sectional area reference values for peripheral nerve ultrasound in adults: a systematic review and meta-analysis—Part I: Upper extremity nerves. Eur. J. Neurol. 28, 1684–1691. https://doi.org/10.1111/ene.14759

Gavriilaki, M., Chatzikyriakou, E., Moschou, M., Arnaoutoglou, M., Sakellari, I., Kimiskidis, V.K., 2023. Therapeutic Biomarkers in Friedreich's Ataxia: a Systematic Review and Meta-analysis. The Cerebellum. https://doi.org/10.1007/s12311-023-01621-6

Grimm, A., Heiling, B., Schumacher, U., Witte, O.W., Axer, H., 2014. Ultrasound differentiation of axonal and demyelinating neuropathies: Ultrasound in Polyneuropathy. Muscle Nerve 50, 976–983. https://doi.org/10.1002/mus.24238

Grimm, A., Schubert, V., Axer, H., Ziemann, U., 2017. Giant nerves in chronic inflammatory polyradiculoneuropathy: Giant Nerves in CIDP. Muscle Nerve 55, 285–289. https://doi.org/10.1002/mus.25272

Kimura J, 2006. Peripheral nerve diseases, handbook of clinical neurophysiology. 2006; Amsterdam: Elsevier., in: Peripheral Nerve Diseases, Handbook of Clinical Neurophysiology. 2006; Amsterdam: Elsevier. Elsevier.

Koeppen, A.H., 2011. Friedreich's ataxia: Pathology, pathogenesis, and molecular genetics. J. Neurol. Sci. 303, 1–12. https://doi.org/10.1016/j.jns.2011.01.010

Leadbetter, R., Weatherall, M., Pelosi, L., 2019. Nerve ultrasound as a diagnostic tool for sensory neuronopathy in spinocerebellar ataxia syndrome. Clin. Neurophysiol. 130, 568–572. https://doi.org/10.1016/j.clinph.2018.12.010

Leonardi, L., Di Pietro, G., Di Pasquale, A., Vanoli, F., Fionda, L., Garibaldi, M., Galosi, E., Alfieri, G., Lauletta, A., Morino, S., Salvetti, M., Truini, A., Antonini, G., 2022. High-resolution ultrasound of peripheral nerves in late-onset hereditary transthyretin amyloidosis with polyneuropathy: similarities and differences with CIDP. Neurol. Sci. 43, 3387–3394. https://doi.org/10.1007/s10072-021-05749-3

Lu, C., Schoenfeld, R., Shan, Y., Tsai, H.-J., Hammock, B., Cortopassi, G., 2009. Frataxin deficiency induces Schwann cell inflammation and death. Biochim. Biophys. Acta BBA - Mol. Basis Dis. 1792, 1052–1061. https://doi.org/10.1016/j.bbadis.2009.07.011

Lucchetta, M., Pazzaglia, C., Granata, G., Briani, C., Padua, L., 2011. Ultrasound evaluation of peripheral neuropathy in POEMS syndrome: US in POEMS Neuropathy. Muscle Nerve 44, 868–872. https://doi.org/10.1002/mus.22258

Lynch, D.R., Farmer, J.M., Tsou, A.Y., Perlman, S., Subramony, S.H., Gomez, C.M., Ashizawa, T., Wilmot, G.R., Wilson, R.B., Balcer, L.J., 2006. Measuring Friedreich ataxia: Complementary features of examination and performance measures. Neurology 66, 1711–1716. https://doi.org/10.1212/01.wnl.0000218155.46739.90

McLeod, J.G., 1971. An electrophysiological and pathological study of peripheral nerves in Friedreich's ataxia. J. Neurol. Sci. 12, 333–349. https://doi.org/10.1016/0022-510X(71)90067-0

Merkies, I.S.J., Schmitz, P.I.M., van der Meche, F.G.A., van Doorn, P.A., 2000. Psychometric evaluation of a new sensory scale in immune-mediated polyneuropathies. Neurology 54, 943–949. https://doi.org/10.1212/WNL.54.4.943

Mulroy, E., Pelosi, L., Leadbetter, R., Joshi, P., Rodrigues, M., Mossman, S., Kilfoyle, D., Roxburgh, R., 2018. Peripheral nerve ultrasound in Friedreich ataxia: Nerve Ultrasound in Friedreich Ataxia. Muscle Nerve 57, 852–856. https://doi.org/10.1002/mus.26012

Rummey, C., Corben, L.A., Delatycki, M., Wilmot, G., Subramony, S.H., Corti, M., Bushara, K., Duquette, A., Gomez, C., Hoyle, J.C., Roxburgh, R., Seeberger, L., Yoon, G., Mathews, K., Zesiewicz, T., Perlman, S., Lynch, D.R., 2022. Natural History of Friedreich Ataxia: Heterogeneity of Neurologic Progression and Consequences for Clinical Trial Design. Neurology 99, e1499–e1510. https://doi.org/10.1212/WNL.0000000000200913

Salvalaggio, A., Cacciavillani, M., Lucchetta, M., Manara, R., Gasparotti, R., Briani, C., 2015. Unexpected nerve neuroimaging findings in Friedreich's ataxia. Clin. Neurophysiol. 126, 1058–1061. https://doi.org/10.1016/j.clinph.2014.08.014

Salvalaggio, A., Coraci, D., Cacciavillani, M., Obici, L., Mazzeo, A., Luigetti, M., Pastorelli, F., Grandis, M., Cavallaro, T., Bisogni, G., Lozza, A., Gemelli, C., Gentile, L., Ermani, M., Fabrizi, G.M., Plasmati, R., Campagnolo, M., Castellani, F., Gasparotti, R., Martinoli, C., Padua, L., Briani,

C., 2020. Nerve ultrasound in hereditary transthyretin amyloidosis: red flags and possible progression biomarkers. J. Neurol. https://doi.org/10.1007/s00415-020-10127-8

van Alfen, N., 2019. Nerve ultrasound in dorsal root ganglion disorders: Smaller nerves lead to bigger insights. Clin. Neurophysiol. 130, 550–551. https://doi.org/10.1016/j.clinph.2019.01.004

Walker, F.O., 2017. Ultrasonography in Peripheral Nervous System Diagnosis: Contin. Lifelong Learn. Neurol. 23, 1276–1294. https://doi.org/10.1212/CON.0000000000000522

Yabe, I., Matsushima, M., Soma, H., Basri, R., Sasaki, H., 2008. Usefulness of the Scale for Assessment and Rating of Ataxia (SARA). J. Neurol. Sci. 266, 164–166. https://doi.org/10.1016/j.jns.2007.09.021

Zesiewicz, T.A., Hancock, J., Ghanekar, S.D., Kuo, S.-H., Dohse, C.A., Vega, J., 2020. Emerging therapies in Friedreich's Ataxia. Expert Rev. Neurother. 20, 1215–1228. https://doi.org/10.1080/14737175.2020.1821654

Study 3. Muscle ultrasound in Inclusion Body Myositis

Abstract

Objective: In this study we aim to investigate the utility of muscle ultrasound in IBM. Exploring the relationship between clinical and neurosonological data in this progressive rare muscular disease could improve both diagnosis and follow-up.

Methods: We prospectively enrolled 10 consecutive patients diagnosed with Inclusion Body Myositis (IBM) and 20 healthy controls. All the patients underwent a complete neurological evaluation with the assessment of muscle strength with the Medical Research Council (MRC) score, anamnestic data (age, sex, disease duration, comorbidities), Body Mass Index (BMI) assessment, and muscle ultrasound. Both quantitative and qualitative score for the following muscles were assessed: first dorsal interosseous, flexor digitorum profundus, biceps brachii, vastus lateralis, rectus femoris, tibialis anterior, medial and lateral gastrocnemius.

Results: Echo intensity was higher in most of the examined muscles (flexor digitorum profundus, biceps brachii, vastus lateralis, rectus femoris, tibialis anterior and medial gastrocnemius) in IBM compared to controls. Muscle ultrasound findings correlate with clinical measures (the higher the muscle echo intensity/Heckmatt score the lower the MRC score of the explored muscle).

Conclusions: Muscle ultrasound can detect muscle abnormalities in IBM, it can detect the pattern of muscle involvement and provide useful objective measures that correlate with clinically assessed scales.

1. Introduction

Inclusion Body Myositis (IBM) is the most common inflammatory myopathy, it is a progressive sporadic disease characterized by a subtle presentation, for this reason the diagnosis may often be challenging. Currently, the diagnosis of IBM relies on a combination of clinical, laboratory, and pathological findings, although these factors may not always provide conclusive evidences (Karvelas et al., 2019) (Weihl, 2019).

Several studies supported the notion that muscular ultrasound may be applied as a diagnostic tool for IBM and could potentially differentiate IBM from disease mimics, yet the wide heterogeneity of the available findings and the different study designs limit its routine use in clinical practice (Abdelnaby et al., 2022; Leeuwenberg et al., 2020).

In this prospective observational study, we aim to investigate the utility of muscle ultrasound in IBM. Exploring the relationship between clinical and neurosonological characteristics in this rare disease could be of particular interest as an easy to perform reproducible marker of disease severity and progression.

2. Methods

Ten consecutive patients with a defined diagnosis of IBM (all the patients had undergone a muscle biopsy) and 20 healthy controls were enrolled. All the patients underwent a complete neurological evaluation with assessment of muscle strength with the Medical Research Council (MRC) score (Kleyweg RP et al., 1991), anamnestic data (age, sex, disease duration, comorbidities), Body Mass Index (BMI) assessment, and muscle ultrasound findings were collected in the same session.

Muscle Ultrasound (Siemens S2000, 9L4 linear probe, Virtual Touch IQ, linear probes 6-16 MHz) was performed following a rigorous protocol, system-settings were kept constant throughout the study. With the patient comfortably lying supine, the following muscles were scanned bilaterally: first dorsal interosseous, flexor digitorum profundus, biceps brachii, vastus lateralis, rectus femoris, tibialis anterior, medial and lateral gastrocnemius. All ultrasound images were acquired in the transverse plane, and all muscles were imaged at a fixed anatomical site (maximal muscle diameter). Every muscle was scanned two times with the transducer held perpendicular to the underlying bone

or fascia. The acquired images were processed offline with a dedicated software (Quantitative Muscle Imaging Analysis, QUMIA, Radboudumc), that allows to draw a region of interest. For gray-scale analysis the average value of two acquired images was then calculated (grayscale value 0 (black)–255 (withe)). To visually score the severity of involvement of the examined muscles we used the semi-quantitative Heckmatt scale (1 normal, 2 increased muscle echo intensity with distinct bone echo, 3 marked increased muscle echo intensity with a reduced bone echo, 4 very strong muscle echo and complete loss of bone echo) (Heckmatt et al., 1982).

Informed consent was obtained from all participants. The research adhered to the principles of the Declaration of Helsinki and its later amendments, and it received approval from the institutional ethics committee.

3. Statistical analysis

Since most variables had a non-normal distribution as assessed by the D'Agostino and Pearson test we used nonparametric tests. Fisher's exact test was used to test the association between categorical variables. The Mann-Whitney test was used to assess differences in continuous variables compared to values found in healthy subjects. Muscle echogenicity between IBM and controls was compared by Kruskal-Wallis test with Dunn's multiple comparison test. The association between clinical and ultrasound findings was assessed by Spearman correlation. Statistical analyses were performed with GraphPad Prism 10.0 (GraphPad Software, Inc., San Diego, CA). Two-tailed p-values <0.05 was considered significant in all analyses.

3. Results

Ten IBM patients (4 males and 6 females) with median age of 65 years (IQR 55.50 – 70.25) and mean BMI 22.37 (SD 2.54) and 20 healthy subjects (9 males and 11 females), with median age of 60 years (IQR 54–66.25) and mean BMI of 21.5 (SD 2.4), were included in this study. The two groups had comparable median age and BMI values. The median disease duration was 8 years (IQR 4.5-9.2).

A total 480 muscle were evaluated (160 in IBM, 320 in healthy subjects) with ultrasound.

In IBM patients we observed a significant inverse correlation between MRC score and both muscle echo intensity and the Heckmatt score ($p<0.0001$ r -0.37 and $p<0.0001$ r -0.42 respectively).

Several muscles in IBM patients showed a significant increase in echo intensity compared to the homologous muscles in healthy subjects at the level of the flexor digitorum profundus, biceps brachii, vastus lateralis, rectus femoris, tibialis anterior and medial gastrocnemius (Figure 1) (Table 1).

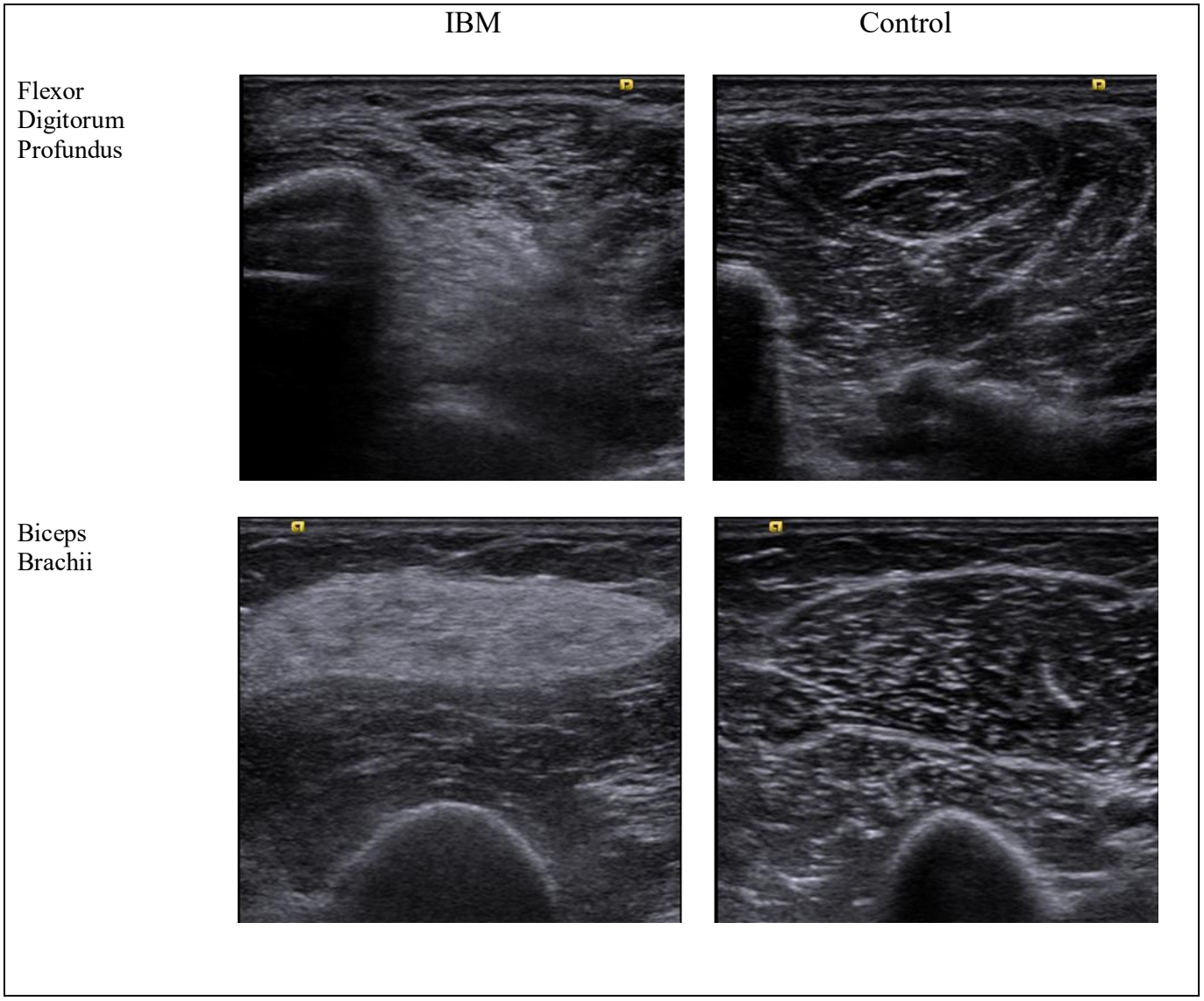

Vastus Lateralis

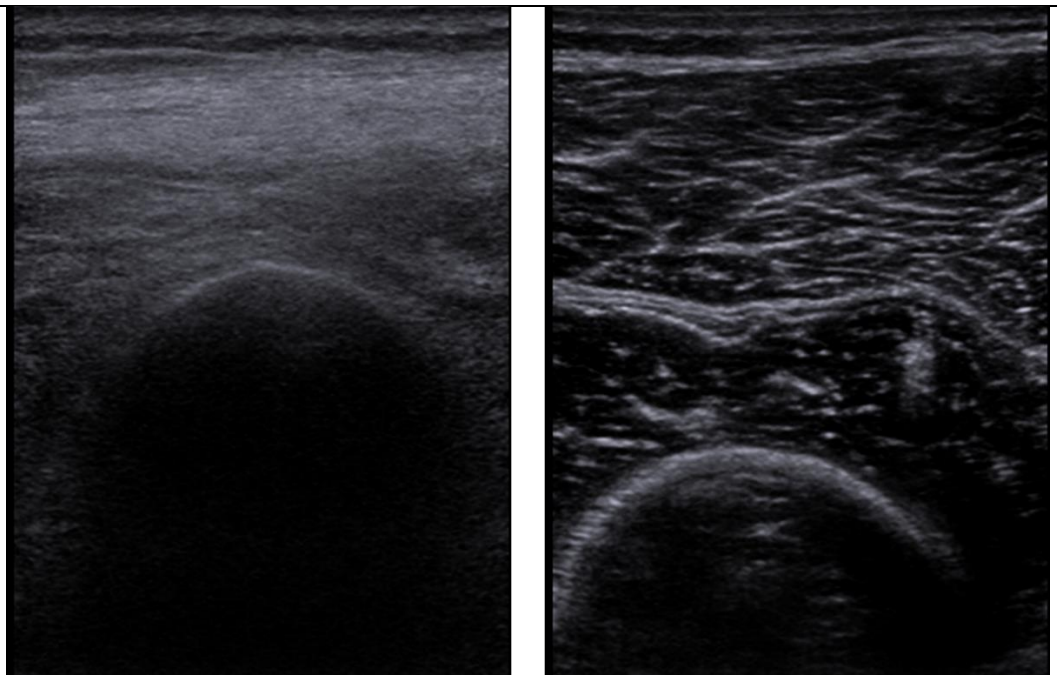

Rectus Femoris

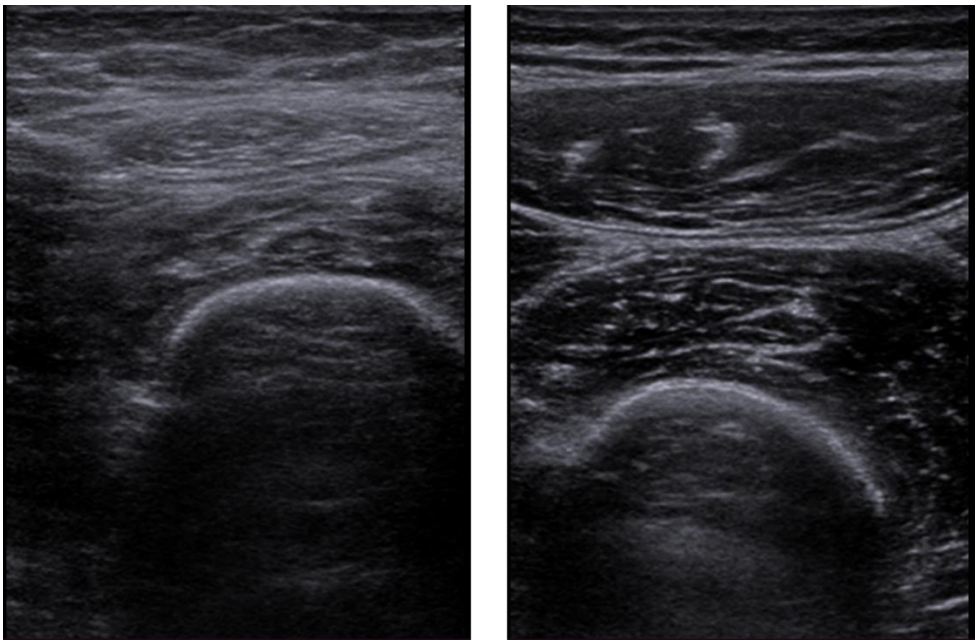

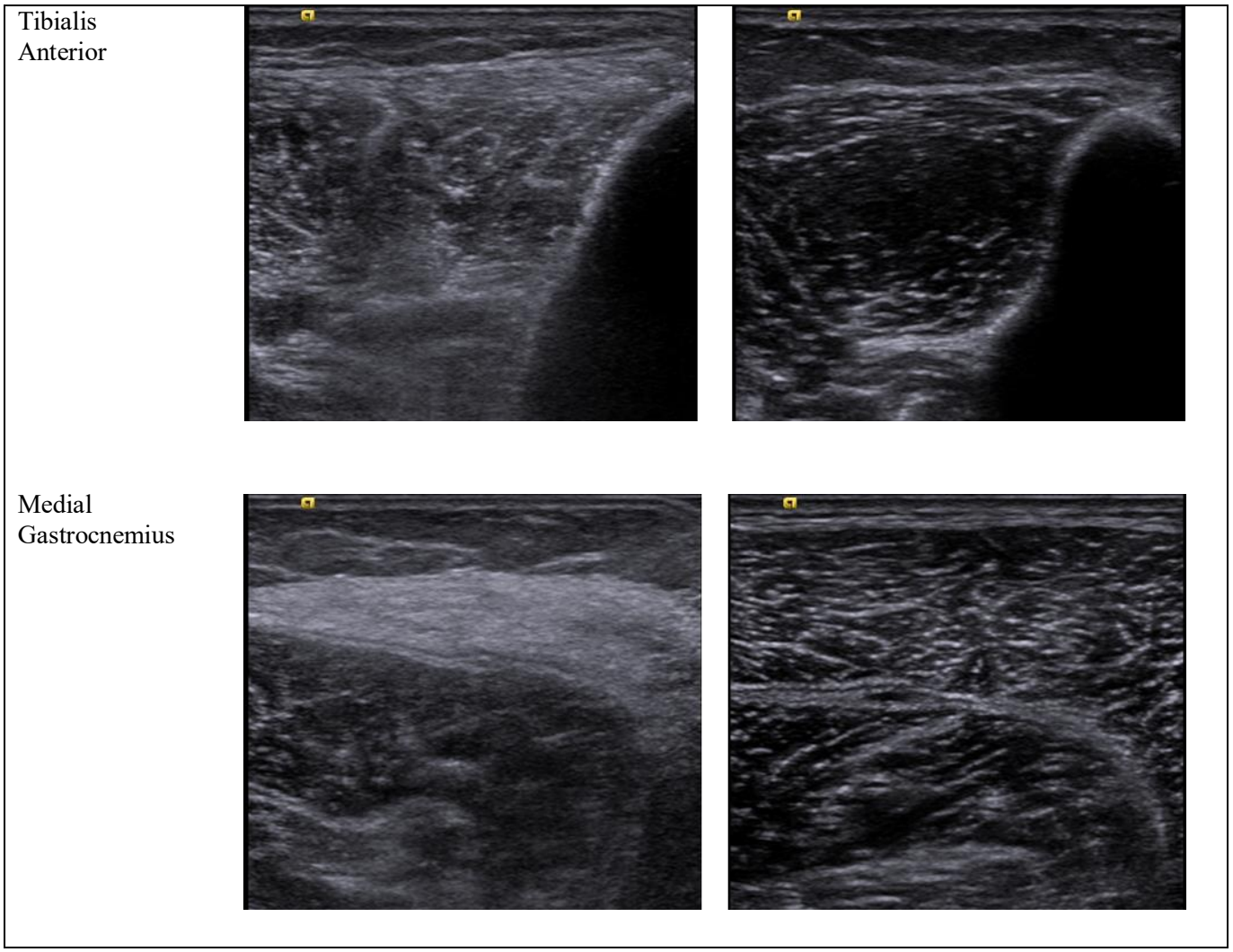

Figure 1. Muscle ultrasound examination showing the most affected muscles in a representative IBM patient and a control.

4 Discussion

Our study confirmed the pattern of muscle involvement found in previous muscle imaging studies in IBM (Abdelnaby et al., 2022) (Vu and Cartwright, 2016). We also observed a correlation between clinical and muscle ultrasound findings.

Despite the numerous attempts targeting both inflammatory and degenerative pathways involved in IBM there are no effective therapies for this rare progressive disease (Naddaf et al., 2018). While new treatment strategies are under investigation (Benveniste et al., 2021), a better understanding of the

available tools for an early diagnosis and an accurate disease monitoring could potentially improve the way we will manage this condition in the near future.

In our study, in line with previous observations (Abdelnaby et al. 2022), we observed a significant higher muscle echo intensity in IBM patients. This finding has been primarily attributed to fatty degeneration; the muscle replacement with fat results in an increased number of reflections within the muscle and alters its acoustic impedance (Guimaraes et al., 2021). This finding is particularly valuable, because while the availability of other neuroimaging tools (i.e. muscle MRI) is limited in many centres, muscle ultrasound is a fast technique which can provide important clinical and diagnostic information. Moreover, muscle ultrasound data correlates with muscle strength as assessed by MRC score (the higher the echo intensity the lower the MRC score of the muscle), thus suggesting the potential use of muscle ultrasound as an objective measure for monitoring disease progression.

Our results regarding visual and quantitative muscle ultrasound support the notion of the good correlation between these two analysis (Wijntjes et al., 2022). Visual and quantitative muscle ultrasound can be considered as complementary methods. While visual score is less time consuming and feasible for a fast assessment of multiple muscles, quantitative muscle ultrasound is able to provide more reproducible muscle ultrasound findings (Arts et al., 2010) (Wijntjes et al., 2022).

Our study has several limitations, first of all the small size of our cohort and the possible technical bias of muscular ultrasound due to its operator-dependency. To hamper this limitation, in our study we applied a strict ultrasound scanning protocol including a control population. Further studies with wider samples combining muscle ultrasound, MRI and histopathological findings are needed to provide a better insight into the applicability of muscle ultrasound in IBM.

5 Conclusions

Muscle ultrasound can detect muscle abnormalities in IBM, it can identify the pattern of muscle involvement and provide useful objective measures that correlate with clinically assessed scales. Our results support the use of muscle ultrasound as a diagnostic tool in IBM.

Table 1. Quantitative muscle ultrasound findings (grayscale values).

Muscle	IBM		Controls		p*
	Median	IQR	Median	IQR	
First Dorsal Interosseous	24.96	20-34.38	14.66	11.43-18	0.148
Flexor Digitorum Profundus	54.39	43.42-65.67	30.21	26.5-33	0.006
Biceps Brachii	63.57	47.51-76.54	31.01	27.52-38	0.0003
Vastus Lateralis	69.53	51.89-84.85	29.5	27.17-36.46	<0.0001
Rectus Femoris	79.99	63.85-85.65	32.23	28.13-33.94	<0.0001
Tibialis Anterior	68.75	50.87-73.21	32.27	27.25-36.35	0.0001
Medial Gastrocnemius	74.27	58.61-90.36	34.74	29.9-37.7	0.0003
Lateral Gastrocnemius	53.92	46.23-80.33	34.87	32.05-37.03	0.0657

*by Kruskal-Wallis test with Dunn's multiple comparison test

References

Abdelnaby, R., Mohamed, K.A., Elgenidy, A., Sonbol, Y.T., Bedewy, M.M., Aboutaleb, A.M., Ebrahim, M.A., Maallem, I., Dardeer, K.T., Heikal, H.A., Gawish, H.M., Zschüntzsch, J., 2022. Muscle Sonography in Inclusion Body Myositis: A Systematic Review and Meta-Analysis of 944 Measurements. Cells 11, 600. https://doi.org/10.3390/cells11040600

Arts, I.M.P., Pillen, S., Schelhaas, H.J., Overeem, S., Zwarts, M.J., 2010. Normal values for quantitative muscle ultrasonography in adults. Muscle Nerve 41, 32–41. https://doi.org/10.1002/mus.21458

Benveniste, O., Hogrel, J.-Y., Belin, L., Annoussamy, M., Bachasson, D., Rigolet, A., Laforet, P., Dzangué-Tchoupou, G., Salem, J.-E., Nguyen, L.S., Stojkovic, T., Zahr, N., Hervier, B., Landon-Cardinal, O., Behin, A., Guilloux, E., Reyngoudt, H., Amelin, D., Uruha, A., Mariampillai, K., Marty, B., Eymard, B., Hulot, J.-S., Greenberg, S.A., Carlier, P.G., Allenbach, Y., 2021. Sirolimus for treatment of patients with inclusion body myositis: a randomised, double-blind, placebo-

controlled, proof-of-concept, phase 2b trial. Lancet Rheumatol. 3, e40–e48. https://doi.org/10.1016/S2665-9913(20)30280-0

Guimaraes, J.B., Cavalcante, W.C.P., Cruz, I.A.N., Nico, M.A., Filho, A.G.O., Da Silva, A.M.S., Zanoteli, E., 2021. Musculoskeletal Ultrasound in Inclusion Body Myositis: A Comparative Study with Magnetic Resonance Imaging. Ultrasound Med. Biol. 47, 2186–2192. https://doi.org/10.1016/j.ultrasmedbio.2021.04.019

Karvelas, K.R., Xiao, T., Langefeld, C.D., Walker, F.O., Pathak, S., Caress, J.B., Baute, V., Cartwright, M.S., 2019. Assessing the accuracy of neuromuscular ultrasound for inclusion body myositis. Muscle Nerve 59, 478–481. https://doi.org/10.1002/mus.26411

Leeuwenberg, K.E., Alfen, N., Christopher-Stine, L., Paik, J.J., Tiniakou, E., Mecoli, C., Doorduin, J., Saris, C.G.J., Albayda, J., 2020. Ultrasound can differentiate inclusion body myositis from disease mimics. Muscle Nerve 61, 783–788. https://doi.org/10.1002/mus.26875

Naddaf, E., Barohn, R.J., Dimachkie, M.M., 2018. Inclusion Body Myositis: Update on Pathogenesis and Treatment. Neurotherapeutics 15, 995–1005. https://doi.org/10.1007/s13311-018-0658-8

Vu, Q., Cartwright, M., 2016. Neuromuscular ultrasound in the evaluation of inclusion body myositis. BMJ Case Rep. bcr2016217440. https://doi.org/10.1136/bcr-2016-217440

Weihl, C.C., 2019. Sporadic Inclusion Body Myositis and Other Rimmed Vacuolar Myopathies: Contin. Lifelong Learn. Neurol. 25, 1586–1598. https://doi.org/10.1212/CON.0000000000000790

Wijntjes, J., Van Der Hoeven, J., Saris, C.G.J., Doorduin, J., Van Alfen, N., 2022. Visual versus quantitative analysis of muscle ultrasound in neuromuscular disease. Muscle Nerve 66, 253–261. https://doi.org/10.1002/mus.27669